Langmuir

Subscriber access provided by CMU Libraries - http://library.cmich.edu

Invited Feature Article

Reconstructive Phase Transition in Ultrashort Peptide Nanostructures and Induced Visible Photoluminescence

Amir Handelman, Natalia Kuritz, Amir Natan, and Gil Rosenman

Langmuir, **Just Accepted Manuscript** • DOI: 10.1021/acs.langmuir.5b02784 • Publication Date (Web): 23 Oct 2015

Reconstructive Phase Transition in Ultrashort Peptide Nanostructures and Induced Visible Photoluminescence

Amir Handelman[1*], Natalia Kuritz[2], Amir Natan[2] and Gil Rosenman[2*]

[1]Department of Electrical Engineering, Faculty of Engineering, Holon Institute of Technology, 52 Golumb st. Holon, Israel.

*Correspondence to Amir Handelman; handelmana@hit.ac.il

[2]School of Electrical Engineering-Physical Electronics, Faculty of Engineering, Tel Aviv University, Ramat Aviv, 69978 Tel Aviv.

*Correspondence to Gil Rosenman; rgil@post.tau.ac.il

Abstract

Reconstructive phase transition has been found and studied in ultrashort di- and tripeptide nanostructures, self-assembled from biomolecules of different compositions and origin, such as aromatic, aliphatic, linear and cyclic (linear FF-diphenylalanine; linear LL-dileucine; FFF-triphenylalanine, cyclic FF-diphenylalanine). The native linear aromatic FF, FFF and aliphatic LL peptide nanoensembles of various shapes (nanotubes, nanospheres) have asymmetric elementary structure and demonstrate nonlinear optical and piezoelectric effects. At elevated temperature, 140-180°C, these native supramolecular structures, (except for native Cyc-FF nanofibers), undergo irreversible thermally-induced transformation via re-assembling into completely new thermodynamically stable phase having nanowire morphology similar to those of amyloid fibrils. This reconstruction process is followed by deep and similar modification at all levels: macroscopic (morphology), molecular, peptide secondary and electronic structures. However, original Cyc-FF nanofibers preserve their native physical properties. The self-fabricated supramolecular fibrillar ensembles exhibit the

FTIR and CD signatures of new antiparallel β-sheet secondary folding with intermolecular hydrogen bonds and centrosymmetric structure. In this phase, the β-sheet nanofibers, irrespective of their native biomolecular origin, do not reveal nonlinear optical and piezoelectric effects, but do exhibit similar profound modification of optoelectronic properties followed by the appearance of visible (blue and green) photoluminescence (PL), which is not observed in the original peptides and their native nanostructures. The observed visible PL effect, ascribed to hydrogen bonds of thermally induced β-sheet secondary structures, has the same physical origin as that of the fluorescence found recently in amyloid fibrils and can be considered an optical signature of β-sheet structures both in biological and bioinspired materials. Such PL centers represent a new class of self-assembled dyes and can be used as intrinsic optical labels in biomedical microscopy as well as for a new generation of novel optoelectronic nanomaterials for emerging nanophotonic applications, such as bio-lasers, biocompatible markers and integrated optics.

1. Introduction. Peptide supramolecular ensembles: secondary structures and their physical properties

The concept of supramolecular chemistry provides a deep insight into the intrinsic architecture of biological structures[1,2]. The multistep natural process of the formation of these nanostructures is governed by molecular-recognition interactions in which the first stage is the self-assembly of peptide/protein biomolecules of elementary building blocks. In the next stage(s), these elementary bio-entities, composed of a few biomolecular units, are self-organized into nano- or microstructures.

This approach, inspired by nature, was successfully applied to the development of man-made nanomaterials composed of chemically synthesized biomolecules. The proposed "Peptide-Lego" principle[3] opened the way to engineering combinations of elementary biological units - amino acids and peptide molecules - into diverse nanostructures (nanotubes, nanofibers, nanotapes, nanospheres, etc), mimicking natural protein fibers[4,5,6]. The model of peptide/protein building blocks kept together by noncovalent bonds[3] in all supramolecular systems and providing their thermodynamic stability, was successfully applied in some pioneering works[7,8,9]. Direct observation of discrete stable diphenylalanine bioorganic dots, which are elementary building blocks, was recently described[10,11].

Supramolecular bioorganic architectures[3,5,7,8,9] are well-organized peptide/protein ensembles packed into diverse biological secondary structures (α-helices, β-turns, β-hairpins, β-sheets, etc)[14]. One of the basic secondary structures is β-sheet, in which the stacking mechanism is based on hydrogen bonds[12,13,14]. Unique physical properties found in β-sheets[29,31] such as the amazingly high mechanical strength of a spider silk[15,16] were ascribed to hydrogen bonds acting as mechanical clamps[17]. The same β-

sheet conformation of the spider silk can also exhibit very high thermal conductivity, 1–2 orders of magnitude higher than that of other proteins[18]. It was also recently reported that the hydrogen bonds of β-sheets of the misfolded amyloid proteins are responsible for a new effect of blue and green fluorescence in amyloid fibrils of different origin[19,20,21], indicating intriguing optoelectronic properties of the β-sheet hydrogen-bonded structure in bioinspired and biological nanostructures.

Extensive research on peptide nanostructures has included investigation of their basic physical properties such as unusually high mechanical rigidity[22], wettability[26,27], as well as ferroelectric[23], piezoelectric[24], nonlinear optical[25], and light-wave-guiding[34] properties. The utilization of these properties with the use of new vacuum-deposition technology[26,27] compatible with microelectronics, indicates promising engineering applications of these advanced bioorganic nanomaterials[3,28,29,30,31] in optoelectronics,[32,33,34,35] peptide-bio-LEDs[36], piezo-electromechanics[37], memory storage[38], electrochemistry[26,29], surface-wettability modification[39,50] and many others.

In this paper we study ultrashort aromatic and aliphatic FF, LL, FFF di- and tri-peptide biomolecular nanostructures of different origin and native conformation by monitoring their basic physical properties during thermally-induced phase transition. We show that this fundamental process found by us in bioorganic systems is governed by thermally activated reconformation of biomolecules or their spatial reconfiguration. Regardless of the origin of di- and tri-peptides and their native architecture, the phase transition takes place by full refolding into another, similar, irreversible and thermodynamically stable fiber-like nanowire morphology with β-sheet structure.

The deep reconstruction found at all levels (molecular, electronic, peptide secondary structure, morphological, etc) provides in this new supramolecular arrangement new physical properties, which are not observed in the original biomolecule monomers and their self-assembled native nanostructures. In the native phase, FF, LL nanotubes and FFF nanospheres possess asymmetric structure and show unique physical properties such as piezoelectric and nonlinear optical effects[23,25,30,24]. In the thermally-induced phase, these ferroelectric phenomena disappear as a result of the newly re-assembled centrosymmetric structure. All these FF, LL and FFF fibrous nanostructures are characterized by the new β-sheet-secondary arrangement, followed by profound modification of the native electronic properties and the appearance of blue/green photoluminescence (PL). This visible PL effect found in ultrashort di- and tri-peptide nanofibers is identical to that recently revealed in amyloid fibrils[20,21] and synthetic bioinspired amyloid-like fibers[19,74,75,76,77]. We assume that it can be considered as an optical signature of β-sheet bioorganic nanostructures.

2. Experimental Section

Sample Preparation and Basic Mode of Studies

From the long list of ultra-short peptide biomolecules, we investigated four different peptide monomers (Bachem, Switzerland): linear aromatic diphenylalanine (FF), cyclic diphenylalanine (Cyc-FF), linear aliphatic dileucine (LL) and linear tri-phenylalanine (FFF). In the native phase, these peptide molecules were self-assembled into various shapes with the use of traditional colloidal technology: linear FF and linear LL were self-assembled into hollow peptide nanotubes (PNT); linear

FFF was self-assembled into nanospheres (PNS) and Cyc-FF was self-assembled into nanofibers.

All the peptide-based native nanostructures were prepared by the following procedure: L-diphenylalanine (FF) peptide (Bachem), L-dileucine (LL) peptide (Bachem), and L-cyclic-diphenylalanine (Cyc-FF) peptide (Bachem), were dissolved in 1,1,1,3,3,3-hexafluoro-2-propanol (HFIP) (Sigma Aldrich) to initial concentrations of 100mg/mL for FF and LL, and 25mg/mL for Cyc-FF, mixed in a vortex mixer (VELP Scientifica) and then further diluted to final concentrations of 2mg/mL in deionized water (for FF PNT, LL PNT and Cyc-FF PNF). FFF PNS was prepared by dissolving the L-triphenylalanine (FFF) peptide (Bachem) in HFIP to an initial concentration of 100mg/mL and then further diluted to a final concentration of 4mg/mL in chloroform. At the end of the fabrication process, four liquid suspensions were obtained: FF PNT, Cyc FF PNF, LL PNT and FFF PNS. Methods and investigation techniques of the physical properties of these native nanostructures are described below in this section.

The next preparation stage was a preliminary heat treatment of the dried native samples to promote thermally induced modifications. It should be noted that all presented experimental data shown for different temperatures were obtained using the following procedure. The peptide samples were gradually heated, step by step, from room temperature to 180°C (at every temperature step the peptides were heated for 1 hour, figure 3 and figure 5) and then cooled back to room temperature. Various physical studies were carried out during this process. We found that up to 180°C, the phase-transition process in the studied peptide nanostructures at any temperature is completely irreversible and all properties acquired during the heating (i.e during phase transition) are frozen and preserved when samples are cooled back to room

temperature. This enables monitoring, in these bioorganic structures, the variation of all physical properties such as molecular state, the secondary structure of the peptide, morphology, optics and more, as functions of temperature throughout the phase-transition process.

Environmental Scanning Electron Microscope (ESEM)

For ESEM measurements, a few droplets of the above self-assembled peptide liquid suspensions were placed on clean silicon substrates and dried at room temperature inside a fume chamber. In order to fabricate the thermally induced FF, LL nanofibers (PNF), FFF PNS, and Cyclic-FF nanofibers, the dried samples were heated in an oven to the required temperature and then cooled to room temperature. All the heated samples were coated with palladium-gold and scanned with the use of a JSM JEOL 6300 scanning electron microscope. It should be noted that although the samples were heated for up to three hours, Figure 1 shows that they were not charred.

Spectrophotometry (Optical Absorption)

The optical-absorption (OA) measurements were performed with a Cary 5000 UV-Vis-NIR spectrophotometer (Varian, a part of Agilent Technologies, USA), over the range of 200-800nm. For the OA measurements, all the peptide-based nanostructures were prepared by the following procedure. For measurements on the native phase, suspensions of the peptide samples in quartz cuvettes (Starna Scientific Ltd., UK), with a path-length of 10mm, were measured directly. In order to fabricate the thermally induced FF and LL nanofibers (PNF), FFF-PNS and Cyclic-FF nanofibers, droplets of the above suspensions were placed on glass cover-slip substrates and dried at room temperature inside a fume-chamber., The dried samples were heated in an oven and then cooled to room temperature. At the end of the fabrication process, four glass substrates for every dried peptide nanostructure were

tested. For the OA measurements, the four peptide samples containing the thermally-induced peptide nanostructures were gently scrubbed into clean quartz cuvettes, which were then filled with deionized water. OA measurements were carried on these water suspensions.

Optical Spectrofluorometry

Measurements of photoluminescence (PL) and photoluminescence excitation (PLE) were performed with the use of a Horiba Jobin Yvon FL3-11 spectrofluorometer. The fabrication procedure for measuring PL and PLE in both native and thermally-induced phases was identical to the fabrication process detailed in the previous section (ESEM), except that for PL/PLE measurements, all the peptide nanofibers were placed on a 1x1cm quartz surface instead of a glass cover slip, and the PL measurements were conducted with a homemade holder for the quartz samples.

Circular-Dichroism (CD) Spectroscopy

Circular-dichroism (CD) spectra were obtained by a Chirascan CD Spectrometer (Applied Photophysics, United Kingdom). The wavelengths, from 190 to 250nm were scanned every four seconds. The fabrication procedure for both native and thermally-induced phases was identical to the fabrication process for the OA measurements. The final water suspensions of all peptide nanostructures were studied.

Time-of-Flight Secondary-Ion Mass Spectroscopy (ToF-SIMS)

The fabrication process of the samples for Tof-SIMS measurements was identical to that mentioned in the ESEM section. All the samples in the native and thermally-induced phase were placed on a clean silicon substrate and measured with a PHI Model 2100 TRIFT II instrument.

Fluorescence Microscopy

Fluorescence images of FF-, LL-, and FFF-nanostructures were obtained with an Olympus BX51WI fixed-stage upright fluorescence microscope. Samples were placed on clean cover slip glass, dried and imaged with X10 Olympus objective. For blue images, a DAPI filter was used, and for green images – a GFP filter.

FTIR measurements

FTIR data were collected with the use of a Bruker Tensor 27 (MA, USA). The fabrication procedure for measuring the FTIR spectra of the samples in both native and thermally-induced phases was identical to the process detailed in the ESEM section. First, a 3x3cm silicon-substrate reference sample was tested. Then, droplets of the peptide suspensions (detailed in the ESEM section) were placed on the silicon substrates and dried at room temperature. After complete dehydration, the FTIR measurements of the native-peptide nanostructures were performed. The peptide samples were then heated to the same temperature over the same time periods, as discussed in the ESEM part. This was followed by cooling and measurement of the FTIR spectra.

Computational details

DFT calculations were carried out with the Vienna Ab initio Simulation Package (VASP)[40] code with Perdew-Burke-Ernzerhof (PBE[41]) and Heyd-Scuseria-Ernzerhof (HSE06) [42] functionals with Van-der-Waals (VdW) correction[43]. We have used projector augmented wave (PAW)[44] pseudopotentials, energy cutoff of 800eV, gamma-point only calculation and a unit cell of 20x20x20 Å. We relaxed the structures until the forces were lower than 0.02 eV/Å. The hydrogen bond stabilization energy is about ~0.2eV per bond (~1eV per FFF dimer), when PBE+VdW functional is used. This energy lowering is compared to that of the isolated monomer and is probably much smaller if compared to monomers in a polar

solvent. However, it is related to the energy barrier for breaking the dimer and indicates stabilization of the hydrogen bonds.

3. Morphology of peptide nanostructures in native and thermally induced phases

3.1 Native phase

At room temperature, the di- and tripeptide biomolecules - linear aromatic diphenylalanine (FF), cyclic diphenylalanine (Cyc-FF), linear aliphatic dileucine, (LL) and linear triphenylalanine, (FFF) were self-assembled into various morphological shapes by colloidal techniques (Figure 1, Native Phase). Linear FF and LL biomolecules were self-assembled in aqueous solution into hollow peptide nanotubes (FF PNT, LL PNT) according to the previously described method[5,9]. Linear FFF biomolecules have nanosphere morphology in chloroform (FFF PNS) and Cyc-FF showed nanofiber structure (Cyc-FF-PNF) in aqueous solution.

Both FF and LL nanotubes have identical open-end tubular architecture in which the length of PNT can reach hundreds of micrometers (>300μm) and the diameter is large (~2μm) (Figure 1 a, c). They consist of the basic monomer amino acids, phenylalanine and leucine, and are stabilized by their hydrophobic side groups[45]. The common hydrophobicity leads to their self-assembly in aqueous solution into similar nanotube shapes. However, aromatic FF residues are involved in π-π stacking interactions[5,9], while LL peptides are self-assembled into nanotubes as a result of intrinsic hydrophobic interactions[45].

The inset images (Figure 1 a, c) show cross-sections of single native FF and LL nanotubes. Their cross-section shapes, hexagonal for FF PNT and orthorhombic for LL PNT, enable their assignment to different crystallographic classes[46]. We assume that the nanoscale self-assembly processes of FF and LL native PNT are governed by

their different molecular-recognition mechanisms - π-π stacking interactions[5,9] for FF and hydrophobic interactions for LL[45], which provide their different crystalline space-group symmetry.

Following these findings, we studied the role of an extra phenylalanine (F) amino-acid unit on the morphology and related physical properties of FFF peptide nanostructures. Previous research showed that the extra aromatic chain and hydrogen-bonding group in FFF leads to plate-like morphology in polar aqueous solution[47], as opposed to linear FF PNT[5,9]. In chloroform, which is a non-polar solvent that we used in our studies, the same FFF monomer creates a sphere-like structure with an average diameter of 2-6μm (Figure 1 e). A similar spherical structure was self-assembled from analogous FFF biomolecules of Boc-FFF[48] under the same environmental conditions during the gradual evaporation of non-polar ethanol solvent under controlled humidity, also showing the influence of the basic solvent parameters on the self-assembly behavior. Another good example of the effect of solvent is the morphology of FF dipeptide nanostructures, which can be changed from tubular to vesicular and 2D-sheets in solvents of different polarity and dielectric constant (ethanol, acetone, methanol, water, chloroform, toluene, and benzene). Such polymorphism can be explained by the nature of the solvent and is defined by specific types of intermolecular interactions (hydrogen bonding, hydrophobic, hydrophilic, etc) between peptide molecules and leads to their specific microscopic morphology[49].

Another category of dipeptide polymorphism was found in nanostructures self-assembled from original Cyc-FF biomolecules at room temperature. In the same aqueous solution in which linear FF creates hollow nanotubes, the Cyc-FF dipeptides revealed a completely different native morphology of nanofibers of tens of μm in

length and 2-3μm in diameter (Figure 1 g). We show below that these Cyc-FF fibers possess unique temperature-stable morphology and molecular conformation. They maintain elementary centrosymmetric organization at temperatures of up to 180°C, unchanged peptide secondary structure and do not show nonlinear optical effects or any visible PL before or after thermal treatment (as opposed to other di-and tri-peptides studied) when subjected to phase transition.

3.2 Thermally-induced phase

Hollow FF-PNT exhibit thermally-induced irreversible phase transition over the temperature range of 140-180°C. This process leads to extreme morphological changes in the normally-aligned FF nanotube structure[50], in which the hollow hexagonal tubes are gradually destroyed, passing into a glass-like state and then transformed into another phase of elongated fiber structures of a shapeless cross section[30].

Horizontally-aligned FF PNT show thermally-induced gradual growing of ultrathin needle-like fibrils, (as is evident from Figure 1b), of diameters in the range of tens to hundreds of nanometers. LL nanotubes undergo a phase transition similar to that of FF PNT. In the same temperature region (T~140-180°C), LL nanotubes drastically change their morphology. Hollow LL PNT (Figure 1c) are rearranged and split into ultrathin fiber-like nanowires of ~400nm in diameter (Figure 1 d). A similar morphological-evolution process was found in tripeptide FFF peptide nanospheres at temperatures of 140-180°C. The FFF PNS (Figure 1 e) are crumpled and open their external shell, exhibiting growth of thin fibers that destroy their native spheres (Figure 1 f).

In comparison with the original linear FF, LL and FFF nanostructures, which underwent extensive morphological reconstruction (Figure 1b-d), Cyclo-FF molecules, self-assembled into fiber-like structures at room temperature (Figure 1g), did not display any detectable modifications after being heated to 180°C, but remained stable, retaining their native morphology (Figure 1h).

Thus, despite the different origin of FF, LL and FFF linear biomolecules and their native morphology of assembled nanostructures (nanotubes, nanospheres), they all undergo similar thermally-induced phase transformation. They pass through re-assembling and full reconstruction into similar nanowire architectures, which have the same morphology as amyloid fibrils[12,14], except the Cyc-FF fiber structure, which retains its morphology over the range of temperatures studied.

It should be noted that all peptide samples were heated gradually, step by step, from room temperature to 180°C through the phase-transition region and then cooled to room temperature followed by measurements of their physical properties. We found that any variations observed during phase transition of morphology, structure, symmetry, optics (optical absorption, photoluminescence), molecular conformation, peptide secondary structure, etc. were completely irreversible. This unique feature of bioorganic nanostructures allowed us to examine their dynamic properties through the phase-transition process. The observed irreversibility is evidence of high thermal stability of this new fibrous-morphology phase (Figure 1).

As we show below, the new stable, fiber-like morphology observed in these ultrashort FF-, LL- and FFF peptide nanostructures, (except for original Cyc-FF), also have signatures of β–sheet peptide secondary structure and PL properties similar to those of amyloid fibrils. These results are consistent with those of basic biomedical research on the mechanism of the folding process of amyloid polypeptides related to

neurodegenerative diseases[12,58]. It has been suggested that amyloid fibrils as well as related non-diseased peptide/protein sequences are self-assembled into the same fiber-like morphology, regardless of their origin. They are stable structures with the lowest thermodynamic state[12,58].

4. Phase transformation in peptide nanoensembles, their structure and properties

4.1 General classification of phase transitions

Deep morphological modification of the peptide nanostructures examined, goes through a full collapse of native open nanotubes or nanospheres to ultrathin fiber-like nanostructures (Figure 1). This irreversible structural evolution indicates a specific and unusual type of phase transition in bioinspired nanomaterials. Solid-state physics considers two basic groups of phase transitions: distortive[54] and reconstructive[51]. The distortive, temperature-driven phase transition is defined by invariable molecular (atomic) composition preserving stable chemical bonds, which can slightly alter their length and orientation by small atomic displacements of 0.01-0.1Å[52]. These transitions are fully reversible when the initial atomic (molecular) disposition (native phase), which changes in the high-temperature phase, is totally restored when the temperature is lowered to below the phase-transition point[52,54]. Another fundamental feature of this phase transition is a group-subgroup symmetry relation, when a low-temperature, low-symmetry phase is a subgroup of a parent high-temperature, high-symmetry phase[51,52,53,54]. These symmetry requirements are observed in ferroelectric phase transitions, and specifically for ferroelectric-paraelectric transitions, which are accompanied by the disappearance of spontaneous electrical polarization[53,54]. In such a case, both ferroelectric-related properties, such as

piezoelectric and nonlinear optical effects of second-harmonic generation (SHG), are not observed if the high-temperature parent phase has a centrosymmetric structure.

The second, reconstructive phase transition is completely different[51]. It involves breaking some of the chemical bonds of the initial, low-temperature phase and is accompanied by an extremely large displacement of atoms[51]. In the reconstructive phase transition, the high- and low-symmetry phases lack a group-subgroup relationship, and the transitions are of the first order[51].

4.2 Reconstructive phase transition, symmetry on the nanoscale and molecular transformation in peptide nanostructures

The profound morphological changes found in FF, LL and FFF nanostructures (Figure 1), constitute the primary evidence that relates them to reconstructive phase transition. The native phase of all these nanostructures undergoes deep re-assembling when FF and LL nanotubes and FFF spheres are transformed into similar nanowire morphology via exceptionally large atomic displacements that reach the micrometer range (Figure 1 a-f). According to the classical solid-state-physics approach[51], such a first-order reconstructive transition could be followed by sharp variation of (a) the elementary nanoscale symmetry of the re-assembled building blocks of these supramolecular nanostructures and (b) breaking (rearrangement) of some of the chemical bonds in the core biomolecules.

(a) Symmetry aspect

Our experimental data (Figure 1a-f) display regular shapes of cross sections of both FF and LL nanotubes in their native phase: FF nanotubes have hexagonal and LL nanotubes, orthorhombic symmetry. Both are related to asymmetric structures where native FF PNTs have hexagonal symmetry $P6_1$ and LL PNTs have orthorhombic

$P2_12_12_1$ symmetry[45, 30,55]. The intrinsic asymmetry of the native phase of dipeptides and tripeptides is the basis for exploration, in these bioinspired nanostructures, of fundamental physical phenomena described by tensors of the third rank, such as piezoelectric, nonlinear optical and linear-optical effects. The experimental observation of piezoelectric and nonlinear optical effects in FF, FFF and LL PNTs was studied in previous works[23,24,25,30]. These studies revealed strong piezoelectricity in FF and LL nanotubes combined with observation of spontaneous electrical polarization oriented along the axis of the tubes[23,24]. The piezoelectric coefficient found for FF nanotubes in the native phase, was close to that of single ferroelectric $LiNbO_3$ crystals[24]. In another research, two-photon nonlinear-optical microscopy was applied to self-assembled phenylalanine-based bioorganic FF- and FFF-peptide nanoensembles of different morphology and asymmetry in the native phase. High nonlinear optical response of second harmonic generation (SHG) was observed[25]. This study led to conclusions concerning strict molecular ordering in aligned-peptide supramolecular structures and the application of these results to nonlinear optical conversion of near-infrared light to green and blue light.[25]

Reconstructive phase transition leads to full atomic rearrangement, recrystallization and repacking of elementary building blocks, followed by variation of the elementary nanocrystalline symmetry. The process of structural transformation was studied in detail for single FF nanotubes[50]. Slow heating led to the closing of the FF nanotube, which gradually lost its hexagonal cross section and was transformed to a shapeless fiber. The elementary symmetry of the FF nanotubes changed from hexagonal symmetry, $P6_1$, to centrosymmetric orthorhombic *Pnma*[50]. In the studied FF, LL and FFF nanofibers (Figure 1 b,d,f), neither piezoelectric nor nonlinear optical effects were observed because of the formation of a centrosymmetric structure[25,30].

This phase transformation leads to a deep reconstruction of the building blocks, changing their symmetry and corresponding physical properties, such as nonlinear optical and piezoelectric effects. We show in the next section, that the new nanowire supramolecular phase has the signature of β-sheet hydrogen bonds and acquires new optoelectronic properties such as visible PL.

(b) Thermally induced molecular transformation

Our experimental data, presented in Figure 2**,** obtained from ToF-SIMS, confirm that the phase transition PNT-to-PNF, for both FF and LL dipeptide nanostructures, is accompanied by irreversible reconstruction of their covalent chemical bonds and the creation of a new type of covalent intermolecular bonds. These experimental studies demonstrate the formation of Cyc-FF and Cyc-LL peptide molecules at elevated temperatures (Figure 2). Such a molecular cyclization process is associated with a loss of water, expressed as a decrease in the molecular weight of FF and LL biomolecules, which make up the building blocks of both phases. The linear-to-cyclic transformation of thermally induced FF PNT was also confirmed by Nuclear Magnetic Resonance (NMR) studies[98]. We assume that the reconformation of thermally-induced biomolecules launches and governs the phase transition in FF and LL nanostructures. Another case is the phase transformation in FFF nanostructures, when FFF nanospheres are reconformed into nanofibers (Figure 1). Investigation of the molecular weight of the FFF biomolecules by ToF-SIMS in the native and thermally-induced phases did not reveal any linear-to-cyclic molecular variation (Figure 2e, f). We believe that the phase reconstruction in FFF nanostructures is defined by spatial reconfiguration of linear FFF molecules followed by the adaptation of another peptide secondary structure and fiber-like morphology, which have different physical properties. Table 1 summarizes these findings.

Thus, deep irreversible transformation in FF, LL and FFF peptide nano-assemblies causes complete collapse of their original structures and the creation of nanofibrous morphologies. Another distinguished feature of any supramolecular bioorganic arrangement is its intrinsic peptide secondary structure when the peptide building blocks fold into one or more specific spatial conformations, driven by a number of noncovalent interactions, such as hydrogen bonding, hydrophobic/hydrophilic interactions, aromatic π-π stacking interactions, electrostatic, van-der-Waals interactions, etc. As we discovered, the reconstructive phase transition can be considered a reassembly process, which leads to newly rebuilt building blocks that acquire different elementary symmetry and physical properties. The phase transformation changes the peptide's secondary structure, strongly modifying its intermolecular noncovalent interactions, followed by deep alteration of optoelectronic properties.

4.3. Native and thermally-induced peptide secondary structures

Peptide self-organization offers unique supramolecular architectures with diverse peptide/protein secondary structures. The most common secondary structures are α-helices and β-sheets, as well as other, less-abundant, structures such as the 3_{10} helix and the p-helix[13,14,31], etc. β-sheets are well known for their ability to assemble into long fibrous structures, as occurs in amyloid fibrils associated with Alzheimer and Parkinson diseases[12,14,58]. Exceptional physical properties of β-sheets found recently, such as high mechanical stiffness and thermal conductivity in spider silk[15,16,17,18] visible fluorescence of amyloid fibrils were ascribed to specific β-sheet secondary structures[19,20,21,74,76,77].

In order to examine the secondary structure of the peptide ensembles in their native and thermally-induced phases that are discussed in this work we applied circular dichroism (CD) [56] and Fourier-transform infrared-spectroscopy (FTIR) methods[57]. CD and FTIR are standard methods for monitoring the conformation kinetics of bioinspired and biological materials[59] and especially for revealing the secondary-structural changes such as detection of β-sheet structures that accompany the formation of amyloid fibrils[12,14,58].

The CD spectra (Figure 3) were measured at room temperature for all self-assembled FF, LL, FFF and Cyc-FF peptide nanostructures. The procedure of the CD test included preliminary heating of the peptide nanoensembles, step by step, from room temperature to 180°C, covering the field of reconstructive phase transition.

For the native phase, the CD spectrum of FF PNT (Figure 3a) exhibits a positive band with two broad peaks of ellipticity. The first maximum of ellipticity is Δε = ~5mdeg at ~218nm, indicative of a n-π^* transition. The second maximum of ellipticity at ~198nm (Δε = ~7.5mdeg) results from a π-π^* transition (energy transition in the amide group)[59]. As the temperature of the preliminary heat treatment is increased, the ellipticity gradually decreases, and at T=~140°C, it crosses a zero line and becomes negative. Finally, at 180°C, a broad negative peak (Δε = -2.2mdeg) at 210nm is observed. Such a change in the circular dichroism reflects a major variation in the structural rearrangement of FF-peptide ensembles and the creation of a new secondary structure[57,59].

In the LL PNT native phase, the CD spectrum shows a single positive Gaussian-shaped band (Figure 3b) with maximum ellipticity of Δε ~ 11mdeg at 230nm, which according to the research[59], corresponds to amide n-π^* transition. This electronic transition typically lies between 210–230nm, and is the lowest energy transition in the

amide group. As the temperature is raised, the measured ellipticity of the peak decreases until, at about 140°C, it changes its sign and is transformed at 180°C into a strong, irreversible negative peak ($\Delta\varepsilon$ = -23mdeg) at 223nm. The inversion of the CD spectrum of LL PNT at elevated temperature is similar to the behavior of FF PNT.

As shown in Figure 3c, the CD peaks of tripeptide nanospheres, FFF PNS, at room temperature in the native phase, exhibit two positive bands with maximum ellipticity at ~199nm and ~217nm and minimum ellipticity at ~209nm. These values are very close to those found in the native FF PNT (Figure 3a). This finding is not surprising since these two positive peaks are well-known indications of π-π stacking of aromatic units[60]. Positive CD bands, observed in the native phase of FF, LL and FFF nanostructures, were also found in proteins, such as Gene5 and avidin[59], and also in many phenylalanine-based nanostructures[61,62,63,64]. The positive CD spectra of FF PNT and FFF PNS (Figure 3) in the native phase are known to be influenced by the aromatic side chains[65]. The results of previous studies, which demonstrated a positive CD spectrum of phenylalanine-based nanostructures were ascribed to a β-turns conformation[63,64]. After heating to elevated temperatures, the CD spectrum of the formed FFF-fibers, becomes negative. This is completely consistent with the behavior of FF and LL nanostructures when they undergo thermally induced phase transition at 140-180°C.

In contrast to the transformation of the ellipticity in the CD bands of FF, LL and FFF nanostructures, the CD spectra of native Cyc-FF-fiber nanostructures are temperature-independent (Figure 3d). They have two negative minima: one at 210nm and the other at 196nm. These minima correspond to n-π^* and π-π^* transitions, respectively[59]. At all temperatures, the sign and ellipticity of the CD bands remains approximately constant and negative. This means that the secondary structure of

synthesized Cyc-FF PNF remains in its native secondary conformation. The thermal stability of cyclic peptides is known to be greater than that of linear peptides[66]. It was suggested, on the basis of FTIR spectroscopy, that the secondary structure of Cyc-FF PNF is most likely attributed to a β-turn or α-helix[67].

Thus, heating at temperatures above 140°C leads to inversion of the sign of CD ellipticity for all the inspected peptide ensembles, except for Cyc-FF fibers, indicating a basic transformation in the secondary structures of these peptides. It should be noted, that at the same temperatures above 140°C, the examined FF, LL and FFF nanostructure peptides also exhibit morphological conformation, acquiring a fiber shape. In addition, FF and LL structures also show a definite molecular linear-to-cyclic peptide reconformation (Figure 1 and Figure 2). The sign of the reversed CD bands found in the spectra of both aromatic FF and FFF nanostructures indicates a chirality reversal. Both FF and FFF nanostructures show negative CD spectra in the thermally-induced phase in the same range of ~210-220nm, which indicates a typical antiparallel β-sheet structure [57,58,59]. The negative CD spectrum that was also recorded for the thermally-induced LL nanofibrils at high temperatures is similar to the CD spectra of other aliphatic peptides[68,69] and can also be related to β-sheet arrangements.

These conclusions are supported by FTIR analysis (Supplementary Materials). The FTIR spectra were studied over the most sensitive spectral region of peptide/protein secondary structures, at wavenumbers of 1600-1700cm^{-1}. This region is related to the amide I vibrational band[70] that allows the revelation of secondary peptide arrangement. Experimental FTIR studies conducted on the four di- and tri-peptides, showed that native nanostructures of FF, LL and FFF peptides subjected to thermally induced phase transition show a similar tendency of deep modification of their FTIR spectra (Supplementary Materials). A new fibrillar phase has significantly

different FTIR frequency structure, which indicates refolding of the original peptide secondary structures. Analysis of these spectra led to the conclusion that the induced fiber phase can be ascribed to β-sheet secondary structure. Self-assembled original Cyclic-FF shows temperature-stable FTIR spectra (Supplementary Materials). These conclusions are completely consistent with morphological and CD data.

It is known that peptide nanostructures are very sensitive to temperature changes that can trigger strong variation in the conformation and secondary structure of the peptide[71]. In our case, thermal treatment of ultrashort peptides (FF, LL and FFF nanostructures) induces reconstructive phase transition accompanied by molecular reconformation of FF and LL biomolecules, sharp changes in the morphology and nanocrystal-structure symmetry. Despite the fact that native FF, LL and FFF nano-architectures are self-assembled by dissimilar intermolecular interactions, all these nanostructures are reassembled and rearranged at elevated temperature into similar amyloid-like fibrous morphology with similar signatures of β-sheet secondary structure (Figure 3). Cyc-FF nanofibers assembled from original Cyc-FF show exceptional stability and have another secondary structure[67]. They do not demonstrate any evolution even after being heated to 180°C.

5. Visible photoluminescence in peptide nanostructure

5.1 Intrinsic visible fluorescence in biological and bioinspired nanostructures

Bioorganic molecules that exhibit intrinsic visible fluorescence, are highly desired in bio-medicine and biotechnology, since they enable tracking and monitoring of basic biological processes both *in-vivo and in-vitro* in cells and tissues. However, the original electronic structure of elementary biomolecules (amino acids, peptides, proteins) does not allow the observation of intrinsic visible photon emission, except

for the unique fluorescent protein of the jellyfish *Aequorea Victoria*, which displays strong absorbance in the blue region and fluorescence of green photon emission with a quantum yield of close to 0.8[72]. The observed native fluorescence of most biomolecules is dominated by residues of the aromatic amino acid tryptophan, which shows UV fluorescence at 350nm. Two other aromatic amino acids - tyrosine and phenylalanine - also show UV fluorescence, at 303nm (for tyrosine) and 282nm (for phenylalanine)[73].

Recent intensive studies are focused on the observation of a new effect of visible fluorescence in biological protein structures, such as disease-related human peptides, amyloid fibrils[20,21,74,] gamma-II crystalline[75], and amyloidogenic *tau* and *lysozyme* proteins related to the human genome and associated with neurodegenerative misfolding diseases[76]. All these aromatic and non-aromatic amyloid fibrils present a similar broadband visible fluorescence peak in the same blue-green spectral range of ~410-520nm when they are excited in the UV or near-UV region. Blue fluorescence was also detected in synthetic bioinspired amyloid-like fibrils formed by amyloid polypeptides, such as elastin-related octapeptide GVGVAGVG[77] and polypeptide (ValGlyGlyLeuGly)[19]. It was found that, regardless of the original biomolecular composition, the amyloid polypeptides show intrinsic fluorescence signatures in the same visible optical range upon assembly into a β-sheet secondary structure. The origin of the observed visible fluorescence was ascribed to electron delocalization via hydrogen bonds in β-sheet structures[20,21,74,75,76,77].

Visible blue PL, at about 450-465nm, was also found in ultrashort FF-dipeptide nanostructures with nanowire morphology[34,36,78,79]. These FF fibrils were fabricated by various methods, such as physical vapor deposition[26,27,29], or by heating native hollow FF nanotubes to temperatures reaching 180°C[30,80]. Blue PL was also

detected in fibrous FF-peptide networks, fabricated at room temperature by introducing aldehyde into the FF-monomers aqueous solution[34].

As was discussed earlier, in the native phase, phenylalanine amino-acid-based FF nanotubes and their derivatives have a PL signature solely in the UV-range at about 290-305nm[36,28]. Blue PL at ~450nm that was found in FF-fiber-like structures, in addition to the native UV PL signal, was attributed to quantum confinement effects[36], and semiconducting properties of FF-cyclic nanowires[29,78].

In previous sections, we have discussed four different ultrashort di- and tripeptide nanostructures assembled from linear FF, FFF, aliphatic LL and Cyc-FF biomolecules. It was found that in the thermally-induced phase, FF, LL and FFF nanostructures are transformed into a fiber-like morphology and change their secondary structure into β-sheets, while native Cyc-FF nanofibers retain their fiber morphology and β-turn arrangement.

In the next section we investigate the optical absorption (OA) and photoluminescence (PL) of these four different aromatic and non-aromatic, linear and cyclic di- and tripeptide nanostructures.

5.2 Optical absorption of di- and tripeptide nanostructures in the native and thermally induced phases

Optical absorption is a direct method for observing photon-electron interactions and studying the electron-energy spectrum. It is an effective tool for fine molecular spectroscopy[73]. Figure 4 depicts the normalized OA spectra of FF, FFF and Cyc-FF nanostructures in both native (dashed line) and thermally-induced phases (solid line). The OA of LL nanostructures in the native phase do not demonstrate any peculiarities. In thermally-induced phase, the OA of LL nanofibers was very weak but pronounced optical anomalies were found with the use of the photoluminescence excitation (PLE)

technique (Figure 6), which is a conventional method that allows one to obtain the same information as the OA method by having a high signal/noise ratio[81].

a. OA in the UV region

The OA spectra can be divided into two regions: the UV range at about 260nm, and a near-UV-visible range beginning from 340nm. It can be seen that in both phases, the three aromatic-amino-acid-based nanostructures (FF PNT, FFF PNS and Cyc-FF PNF) share similar absorption spectra in the UV region, where a strong OA peak appears at ~260nm (Figure 4). Analysis of FF nanotubes shows that this peak is followed by two satellite sub-peaks, located at 265nm (4.68eV) and 253nm (4.90eV), reflecting its fine native structure. The energy intervals between two neighboring peaks are 0.1–0.11eV. The location of these OA peaks is a well-known spectrum probe for the phenylalanine amino-acid unit[73] (inset in Figure 4 a, dashed line, monomer). These UV OA peaks, shown in all the aromatic amino-acid-based nanostructures, maintain their location in the same spectral region for both native and thermally-induced phases (Figure 4). This means that OA in the UV region around 260nm is not influenced by variation of morphology, molecular organization or peptide secondary structure, and can be presented as the invariant optical signature of phenylalanine aromatic residues that make up the building blocks of the aromatic peptide nanostructures.

b. OA in near-UV-visible region, $\lambda \geq 340$nm

As opposed to the previously discussed UV region, the OA spectra in the near-UV-visible region of the FF and FFF aromatic-peptide nanostructures show an extreme modification of the thermally-induced phase (preliminary heating >140°C). OA spectra of both thermally-induced FF and FFF nanostructures have a step-like structure, with a broad hump at ~360nm and also contains another small hump at

~410nm, as clearly seen in Figure 4 and from the insets in Figure 4 a, solid line and Figure 4 b, solid line. Such abnormal OA behavior at 360nm and 410nm was found for thermally-induced FF nanofibers, in which the fiber refolding process is accompanied by molecular transformation of FF-linear to FF-cyclic molecules. It should be noted that Cyc-FF nanofibers assembled at room temperature from originally cyclic FF molecules do not demonstrate any optical anomaly in this region. Thus, these two FF-nanowire morphologies have the same FF-cyclic molecular conformation but their OA spectra are completely different (Figure 4 a, c). This means that newly generated optical absorption at these wavelengths in the thermally-induced FF and FFF fibers (Figure 4 a, b) is not defined by the conformation of the biomolecules and the composition of their building blocks. It can be assumed that optically excited electronic transitions at 360 and 410nm occur from newly created electron-energy levels related to specific peptide secondary organization. We show below that this new electronic structure appears as a result of the formation of intermolecular hydrogen bonds of β-sheet structures alone.

5.3 Photoluminescence in peptide nanostructures

a. PL in the native phase of peptide nanostructures

Following the results of OA, the photoluminescence (PL) and photoluminescence excitation (PLE) spectra were measured both in the native and thermally-induced phases. In the native phase (Figure 5 a), when the aromatic FF nanotubes, FFF nanospheres, and Cyc-FF PNF are excited at ~265nm, similar fluorescence UV photon-emission peaks at ~285-305nm are observed, as opposed to the case of aliphatic LL PNF, which does not show any UV PL photon emission when excited at 265nm. The PL peak at ~285-305nm in FF, FFF, and Cyc-FF PNF is a

well-known optical PL signature of phenylalanine residues[73,74]. Since LL PNF is composed of aliphatic amino acids only, the lack of PL peaks in the UV region around 290nm is predictable.

b. Thermally-induced phase: Visible blue PL excited in UV, λ=265nm

The PL emission spectra, following 265nm excitation in the thermally-induced phase for FF, LL, FFF and Cyc-FF PNF are presented in Figure 5 b. In this new fiber phase, the UV peaks of FF PNF and FFF PNF display a small red shift to 305nm and are aligned with the Cyclo-FF peak, while LL PNF does not show any PL. This result proves that the UV peak at ~305nm results from the aromatic origin of the FF, FFF and Cyc-FF molecules, and not by biomolecule conformation (linear or cyclic), peptide composition (di- and tripeptide) or peptide secondary structure. The second PL blue peak appears at ~460nm only after phase transition of FF and FFF nanofibers. LLfiber nanostructures do not show any blue PL at ~460nm when excited at 265nm because of their non-aromatic origin. Cyc-FF fibers do not show any PL in the visible region.

Figure 5 c presents the PL data as a function of temperature during phase transition for FF-PNT/PNF. The UV PL peak does not change its wavelength (290-305)nm, showing unaltered PL intensity over the whole temperature range (25-180°C). The opposite behavior was found for the blue PL peak at 440-460nm (Figure 5 c). This visible PL peak appears at ~120-140°C only and gradually grows with temperature, showing dynamics of the phase transition and development of a new fiber phase. This blue PL peak reaches its maximum value at about 170°C. It should be noted that the temperature (~140°C) at which the visible blue PL at ~460nm appears, following excitation at 265nm (Figure 5 c), coincides with the temperature at which the CD bands are reversed, indicating reassembly of the native phase of FF

open nanotubes into a thermally induced phase of FF fibers having β-sheet structure (Figure 3 a). These results provide valuable information regarding the origin of this mysterious visible blue PL[36,30,78]. The photon emission in the blue region, after excitation at 265nm, was found in aromatic FF and FFF nanowires (Figure 5 b, c), is not observed in Cyc-FF nanofibers. It can be assumed that the origin of this visible PL peak does not depend on the conformation of the biomolecules, the presence of aromatic residues and water molecules, but is defined by the new electronic structure of β-sheet peptide nanofibrils formed during phase transformation in both FF and FFF fibers.

c. Thermally-induced phase: Visible PL excited at 360nm and 410nm

In the thermally-induced phase, the visible PL effect also appears for non-aromatic LL fibers (Figure 6 a) and it shows a broadband blue PL at about 420-460nm together with blue PL for aromatic FF and FFF nanofibers (excited at 360nm). It was found that for FFF-fiber structures blue PL shows a small red shift toward λ~470-480 when these nanostructures are excited at 360nm (Figure 6 a). Native Cyc-FF nanofibers do not display visible PL for this excitation wavelength either. The appearance of the blue PL peak in various types of peptide nanostructures further strengthens our speculation that the origin of this blue PL peak is not related to the presence of aromatic resides, or conformation of biomolecules from linear to cyclic molecules. This blue PL peak at ~460nm was observed in FF, FFF and LL nanofibers, regardless of the origin of their native amino acid groups (FF and FFF are aromatic and LL is aliphatic).

In addition, these data show that FF, LL and FFF peptide nanofibers could also emit light at the edge of the green region. This is especially pronounced for FFF fibrous structures (wide PL peak with maximum intensity at ~480-510nm when

excited at ~410nm (Figure 6 b). The origin of these two visible blue/green PL emissions could be found from PLE data presented in the insets of Figure 6, which are consistent with OA data (Figure 4). It should be noted that in the native phase, visible PL is not observed in any peptide nanostructures for any excitation wavelength. The bright, glowing peptide-based fiber nanostructures are directly detectable by a fluorescence microscope. Figure 7 shows the observed blue-light emission from the thermally induced aromatic FF and aliphatic LL nanowires and green PL from the aromatic FFF nanostructures.

Several models have been proposed to explain the origin of blue/green light emission from FF-peptide nanostructures. The appearance of blue PL in thermally-induced FF PNF was related to the peptide monomer material, either due to the quantum-confinement effect[36], or affected by the FF molecular-cyclization process[34], which modifies the electronic spectra of Cyc-FF fibers, converting them to semiconductors [29,78.]

In this work we show (Figure 5, Figure 6, Table 1) that blue/green PL does not depend on the origin of peptide molecules or their biomolecular reconformation (linear or cyclic). The only common feature of these visible PLs found in supramolecular FF, LL and FFF structures, self-assembled from different biomolecules, is their β-sheet-peptide secondary structure, which is generated by thermal treatment under refolding of the native phase and reconstruction into a new fiber phase (Figure 1, Figure 3, Supplementary Materials). Extensive modification of their native secondary structure provides new noncovalent bonds in a new secondary structure. The thermally-induced β-sheet secondary folding that is found is characterized by hydrogen bonds having another electronic-energy spectrum compared to the native noncovalent bonds.

As has been mentioned in the previous sections, recent studies reported on the observation of blue-light emission of various biological aromatic and non-aromatic protein and polypeptide amyloid nanofibrous structures[20,21,75,76,77]. All of them, regardless of their native biomolecular composition, have similar nanofiber morphology with extended antiparallel β-sheet structure, showing similar pronounced fluorescence peaks in the blue/green visible range, with maximum intensity at about 440-460nm, when excited almost in the same region of ~355 or ~405nm. Surprisingly, the same visible PL at the same excitation wavelength was found in our study, for ultrashort di-and tripeptide nanostructures subjected to phase transition and also adopting β-sheet arrangement. We believe that bioinspired ultrashort peptide nanostructures and amyloid fibrils[20,21,75,76,77] share similar fundamental optoelectronic properties. Original amyloid fibrils, assembled into β-sheet structures, are stabilized by a network of hydrogen bonds between the basic protein/polypeptide building blocks of the amyloid fibrils[20,21]. As we showed in this work, on measuring visible PL photon emission (Figure 6), β-sheet structures and related hydrogen bonds gradually appear and grow during reconstructive phase transition in FF, LL and FFF nanofibers displaying dynamic formation of β-sheet peptide structures (Figure 3). Thus, these hydrogen bonds are the only common structural feature of these completely different supramolecular natural amyloid fibrils and thermally-induced short synthetic peptide nanowires.

The reconstructive phase transition that was found in the simple aligned peptide aggregations, leads to a new phase of refolded, antiparallel β-sheet nanostructures with a broad network of hydrogen bonds followed by extensive modification of the electronic properties of the native structures. This visible photoluminescence effect, occurring as a result of the photon excitation of low-

energy electronic transitions, is ascribed to the intrinsic electronic structure of the newly assembled β-sheet arrangment[20,21,75,76,77].

6. Possible mechanisms for PL – a theoretical discussion

The relation between the observed phase transition and appearance of OA anomalies and PL in the visible range is very clear from the experimental research performed for ultrashort di- and tri-peptides. These new optical properties found in thermally-induced nanofiber peptide structures are consistent with those revealed in amyloids fibrils when both are assembled into β-sheet secondary structure[20,21,75,76,77]. However, the detailed mechanism of this phenomenon is a theoretical challenge. The assembly of hydrogen-bonded aggregates (H-Aggregates), dimers and other small complexes, was shown to induce PL activity also in other systems such as π-conjugated polypeptides[82,83], anthracene derivatives[84] and others.

There are several mechanisms that are known to affect the optical behavior of such systems. One of them is molecular reorganization, in which the flexibility of the hydrogen bonds allows a significant change of intermolecular distances and orientation during photo-excitation, thus allowing energy transfer and new intermediate electronic states. Such a mechanism was shown to induce a strong change in the optical gap and new PL properties for both intermolecular[85] and intramolecular[86] hydrogen bonded systems.

Organic molecular crystals can also have diverse interactions of electron-hole pairs such as Frenkel and charge-transfer excitons, as was shown for pentacene crystals[87]. Inter-molecular exciton energy transfer is known to affect fluorescence in molecular aggregates and organic crystals and is a possible mechanism here as well. The last mechanism that we consider is the effect of packing on electronic structure. In hydrogen aggregates and *β*-sheets, crystal structure can lead to spatial

configurations where peptide side groups become closer than what was energetically favorable in solution or in other less dense configurations. This can lead to new delocalized electronic states and as a result, reduction of the optical gap. Such an effect was demonstrated with π-conjugated polypeptides[82,83] and with anthracene derivatives[84].

To check the last possibility, we have calculated, with Density Functional Theory (DFT)[88] the electronic structure of both the monomer and different dimers of FFF as a minimalistic model for the inter-molecular effects (see computational details section). One of the calculated dimers is an anti-parallel hydrogen bonded dimer of FFF-molecules (Figure 8), such anti-parallel dimers are also predicted by molecular dynamics (MD) simulations[89,90].

With the DFT Heyd-Scuseria-Ernzerhof (HSE06)[91] functional, the simple hydrogen bonded FFF dimer showed only a small (0.1 eV) band-gap reduction relative to the monomer. This small reduction shows that the effect of delocalization does not occur directly through the hydrogen bond itself. Another dimer orientation that we checked by same method is the case when conjugated side groups are approaching each other (~3.0Å). In such cases, we get a band-gap reduction of 0.5eV but at a cost in energy of about 0.4eV. Such a configuration is not energetically favorable in solution or in other less dense structures but might become more possible in a β-sheet-like densely packed structure. The electronic Density of States (DOS) for both configurations is shown in the supplementary material.

Ground state DFT calculations are known to explain only for a part of the absorption shift[92] and therefore higher-level calculations are needed. The separation of the different possible mechanisms for the hydrogen-bonds effect on OA and PL is an interesting and important challenge for both theory and experiment. Molecular-

reorganization effects can be analyzed with excited state geometry that can be calculated with time-dependent DFT[85,93]. The availability of super-fast spectroscopy methods can help to perform experimental analysis of such possible effects. The analysis of excitonic effects will require calculations beyond standard DFT, and this is possible with calculations of the full Bethe-Salpeter equations[87,94].

7. Conclusions and future development

Thermally-induced reconstructive phase transition found in supramolecular ultrashort di- and tri-peptide native nanostructures of different origin and morphology, reveals a new route for their reassembling to identical thermodynamically stable phase having β-sheet secondary structures with nanowire morphology. These peptide nanofibers demonstrate new and common basic physical properties, among them visible photoluminescence. The induced PL effect does not depend on peptide monomer origin. It is observed in antiparallel β-sheet peptides structures and ascribed to electron transitions induced by the hydrogen bonds connecting these extended β-sheets in the peptide nanofibers. We assume that this phenomenon should be observed in other peptide nanostructures, which are natively rich in β-sheets. It was recently found[95] that short Fmoc-FF peptide hydrogel possessing β-sheet conformation, exhibit a blue-PL peak at 460 nm without any thermal treatment. New biomedical studies also reported on the observation of blue and green photon emission in many biological aromatic and non-aromatic proteins and polypeptides folded into amyloid fibrils having β-sheet structures[20,21,75,76,77]. Thus blue/green PL found in this work in ultrashort peptide nanofibers can be considered an optical signature of a wide range of peptide β-sheets secondary arrangements for both biological and bioinspired nanostructures.

The hydrogen-bonded network responsible for visible PL in β-sheets structures represent a new class of self-assembled visible dyes of biological origin and can be used as bio-labels. Extensive efforts for development of fluorescence visible bio-labels were directed toward imaging of structural organization and basic processes in living cells, for cancer diagnostics, tracking misfolding and aggregation of amyloid proteins responsible for neurodegenerative diseases such as Alzheimer and Parkinson[20,21,75,76,77].

A good example of visible fluorescent biological label is universal genetically encoded Green Fluorescent Protein (GFP) and its homologs extracted from the jellyfish *Aequorea victoria*[96] and from diverse bioluminescent marine animals[72,97]. However the effect of GFP and its homologs is defined by the electronic structure of particular rare proteins. In our work found visible PL of self-assembled dyes formed by hydrogen bonds is completely different. It is related to the common biological or man-made bio-nanostructures folded into β-sheet organization regardless of biological entities. Being excited in amyloid fibrils or synthetic peptide nanowires this PL effect is the basis for a new method of optical recognition of β-sheet peptide nanostructures and monitoring their dynamic aggregation. These new bio-labels can be also used for applications in biomedical research, bio-nanotechnology and diverse nanophotonic devices such as bio-lasers and integrated photonics .

Acknowledgements

We thank Dr. D. Szwarcman and Dr. R. Attali for the helpful discussions and productive ideas.

Figures for Paper

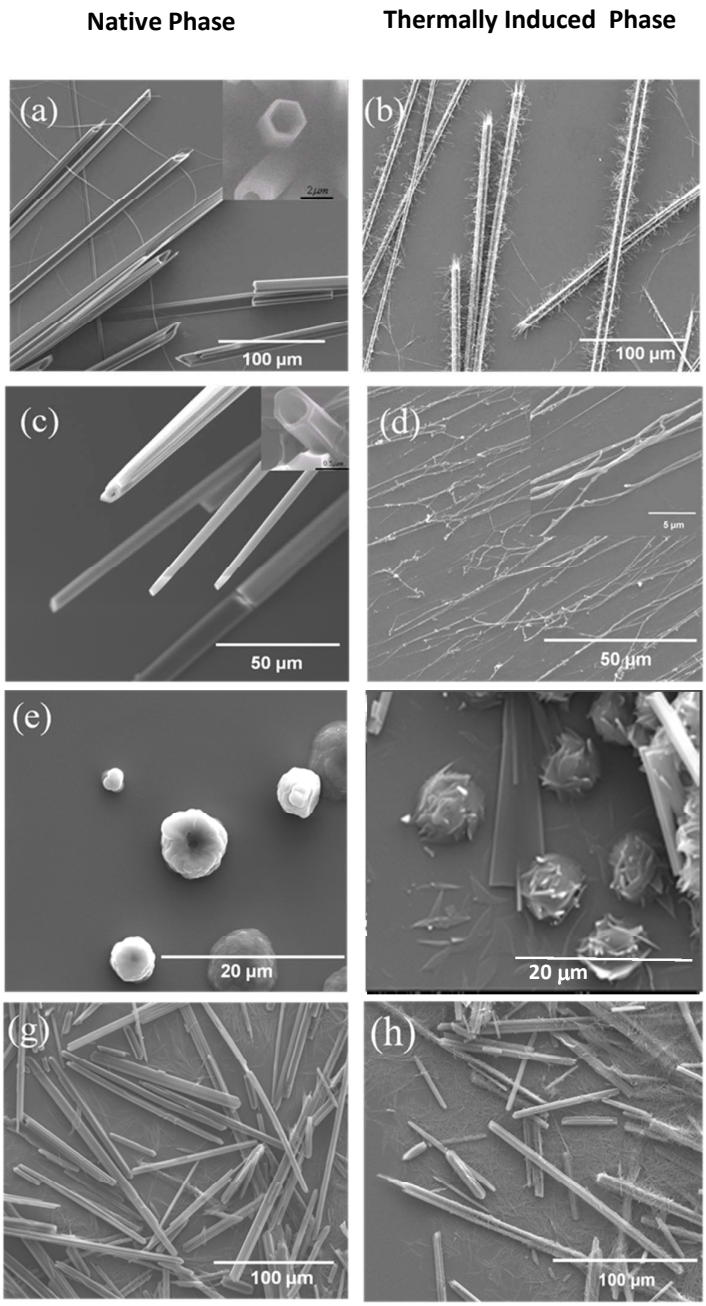

Figure 1. ESEM images:
a) native FF PNT (inset: the cross-sections of hollow FF PNT have pronounced regular shapes allowing to relate them to definite crystallographic class of hexagonal symmetry) ,
b) thermally-induced FF PNF heated to 180°C. The gradual growing into needle-like thin wires-fibrils is clearly seen,
c) native LL PNT (inset: LL PNT cross-section demonstrates orthorhombic symmetry),
d) thermally-induced LL PNF heated to 180°C. Full collapse of hollow nanotubes structure into thin nanoscale wires-like fibrils was found,
e) native FFF PNS,
f) thermally-induced FFF PNS heated to 180°C. The image of the heated FFF PNS demonstrates the gradual growing of fibrils that break out from the sphere-like structures, similarly to the thin fiber structures of FF and LL fibers,
g) native Cyc-FF fibers, h) heated Cyc-FF PNF to 180°C. Note that there is almost no substantial change in the morphology of these fibrous structures.

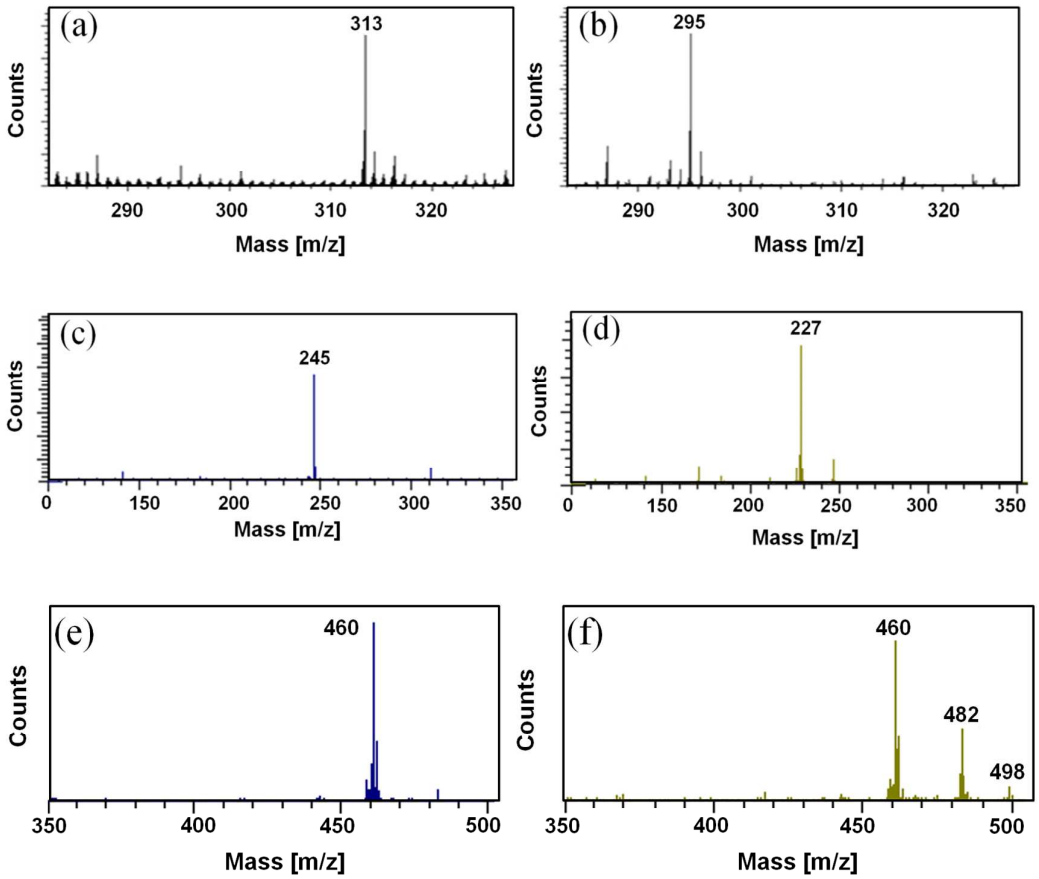

Figure 2. ToF-SIMS of a) native FF-PNT, b) thermally-induced FF-PNF, c) native LL-PNT, d) thermally-induced LL-PNF, e) native FFF-PNS, f)) thermally-induced FFF-PNF. The molecular weight of both FF and LL was reduced after heating by 18 g/mol, corresponding to water loss during linear-to-cyclic molecular transformation. Molecular weight of FFF does not change.

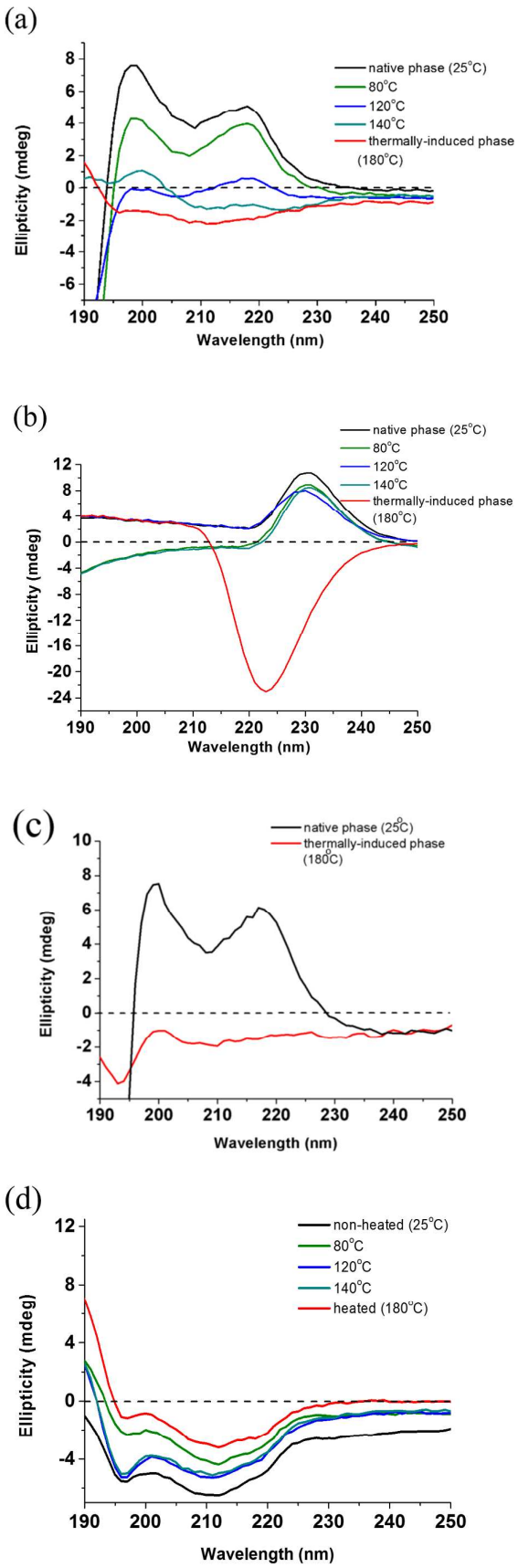
(a)
native phase (25°C)
80°C
120°C
140°C
thermally-induced phase (180°C)
Ellipticity (mdeg)
Wavelength (nm)
(b)
native phase (25°C)
80°C
120°C
140°C
thermally-induced phase (180°C)
Ellipticity (mdeg)
Wavelength (nm)
(c)
native phase (25°C)
thermally-induced phase (180°C)
Ellipticity (mdeg)
Wavelength (nm)
(d)
non-heated (25°C)
80°C
120°C
140°C
heated (180°C)
Ellipticity (mdeg)
Wavelength (nm)

Figure 3. CD spectra vs temperature of the studied di- and tri-peptide nanostructures showing variation of the peptide secondary structure in the region of reconstructive phase transition:

a. FF PNT/PNF ; b. LL PNT/PNF; c. FFF PNS/PNF; d. Cyc-FF PNF

CD spectra show that as the temperature increases, the sign of the ellipticity of FF-, LL and FFF nanostructures changes and becomes negative, suggesting β-turns to β-sheets transition.

CD spectra vs temperature of Cyc-FF fibers remains stable and negative

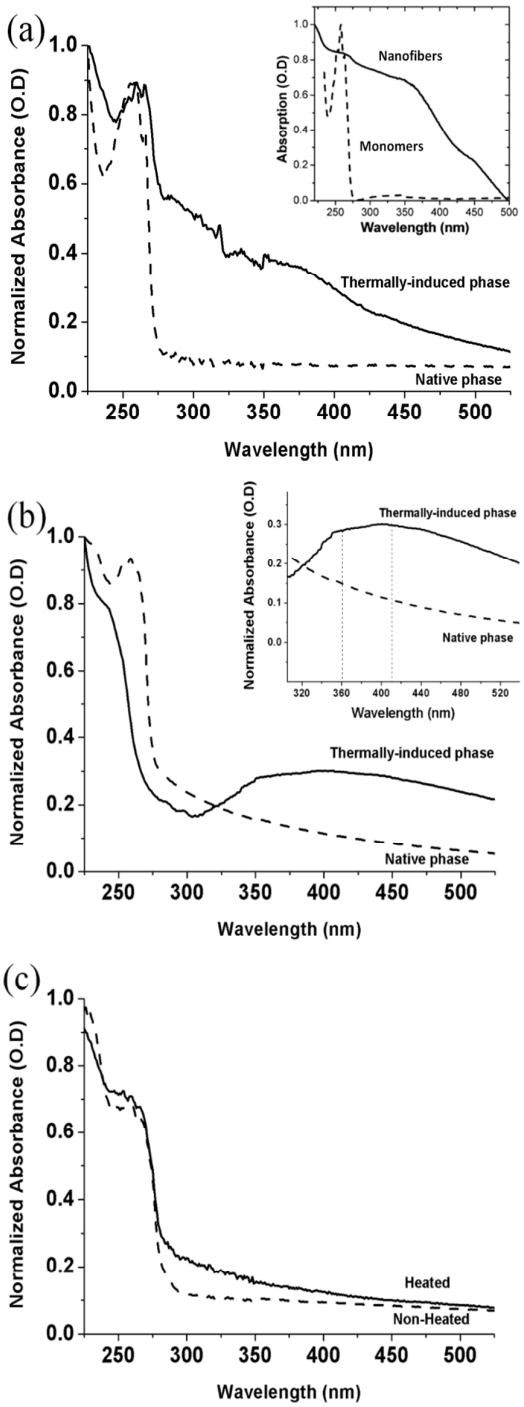

Figure 4. UV-visible normalized optical absorption (OA) spectra of different peptide nanostructures at the native phase (25°C, dashed lines) and at the thermally-induced phase (180°C, solid lines)

UV-visible normalized optical absorption (OA) spectra of different peptide nanostructures at the native phase (25°C, dashed lines) and at the thermally-induced phase (180°C, solid lines)

a) FF PNT/PNF. The inset shows OA from FF PNF deposited by physical vapor deposition technology. This OA spectrum is similar to the OA of FF PNF in the thermally-induced phase.
b) FFF PNS/PNF. The inset depicts an expanded view of the humps at ~360 nm and ~410 nm, visible only at their thermally-induced phase.
c) Cyc-FF PNF heated and non-heated. The absorption spectrum of Cyc-FF PNF does not change during heating.
The OA of LL nanostructures in both native and thermally-induced phases was very weak but pronounced optical anomalies were found using the PLE technique (Figure 6)

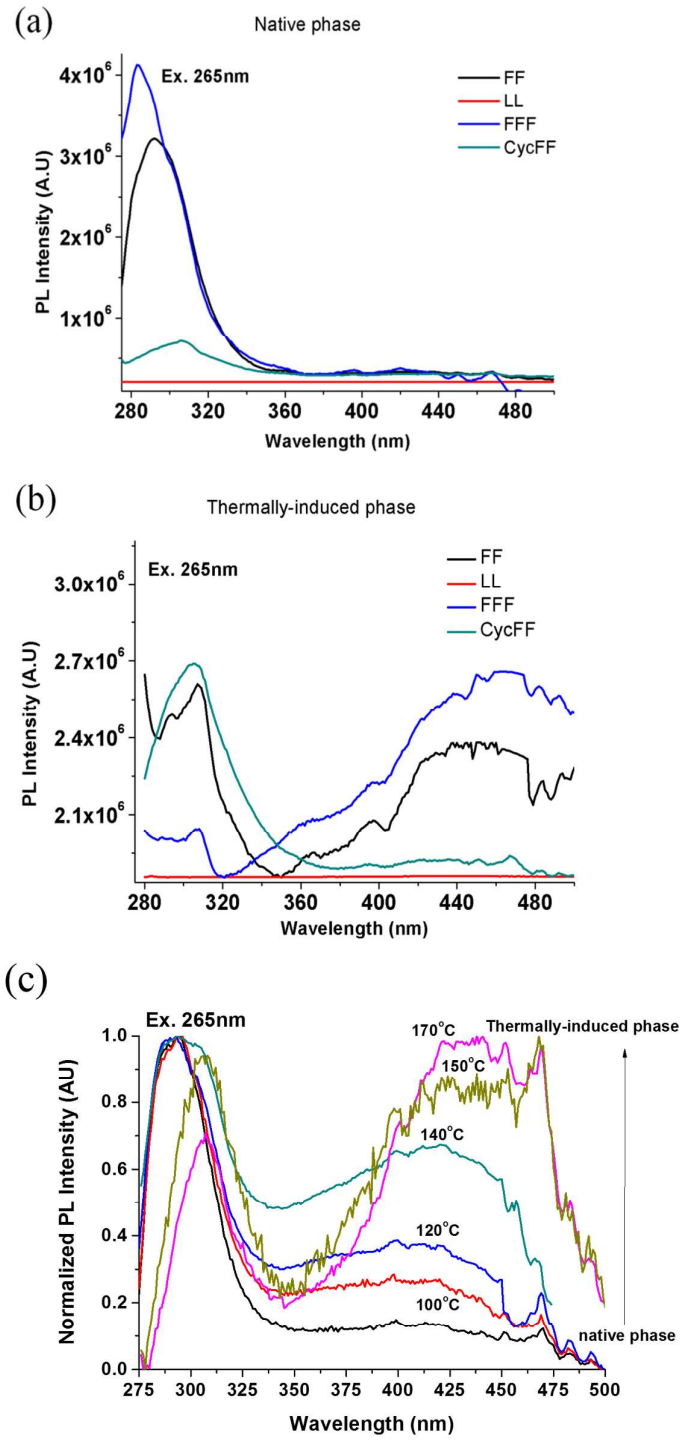

Figure 5. PL spectra in native and thermally-induced phases

a) PL spectra in the native phase (excitation at 265 nm) of FF PNF, LL PNF, FFF PNS, and Cyclo-FF fibrous peptide nanostructures. The aromatic FF, FFF, and Cyc-FF PNF show similar photoluminescence signature at ~285-305 nm. LL-PNF, which does not demonstrate any PL peak when excited at 265 nm since it does not contain aromatic side chains.

b) PL spectra (excitation at 265nm) of FF , LL , FFF nanostructures in the thermally-induced phase, and Cyc-FF fibrous peptide nanostructures. At this phase, the first PL peak almost keeps its position at ~285-305 nm in FF, FFF, and Cyclo-FF

nanostructures. The second blue PL peak appears at 420-460 nm for FF PNF and FFF fibers due to formation of β-sheet peptide secondary structures as opposed to Cyc-FF fibers which does not display visible PL. Non-aromatic LL fibers does not demonstrate visible PL being excited at 265 nm.

c) Dynamics of PL of FF peptide nanotubular structures during thermally-induced phase transition. Stable UV-PL peak is observed as opposed to visible blue PL which gradually grows from T>120°C correlated with formation of β-sheet peptide secondary structure.

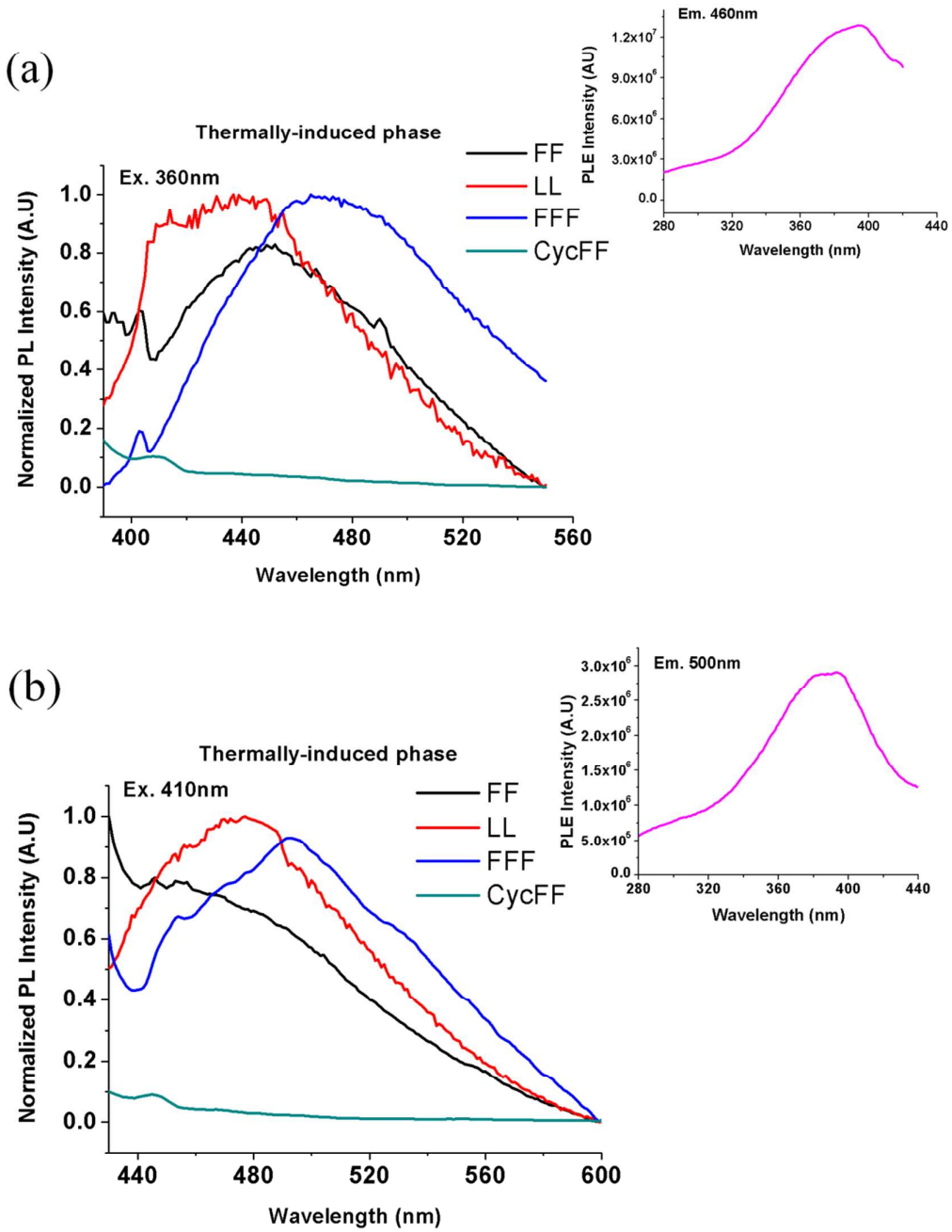

Figure 6. PL and PLE (inset) spectra in the thermally-induced phase of FF, LL and FFF and Cyclo-FF nanofibers.

a) PL blue emission peak observed for FF, LL and FFF nanofibers at ~460 nm when excited at ~360 nm.

b) PL emission observed for FF, LL and FFF nanofibers around ~510 nm when excited at ~410 nm.

PLE spectra, as shown in the insets of (a) and (b) are similar for all peptide fiber nanostructures except for Cyc-FF nanofibers which do not emit any PL in the visible region. It should be noted that at the native phase all these peptide nanostructures do not show any PL peaks in the visible spectral regions.

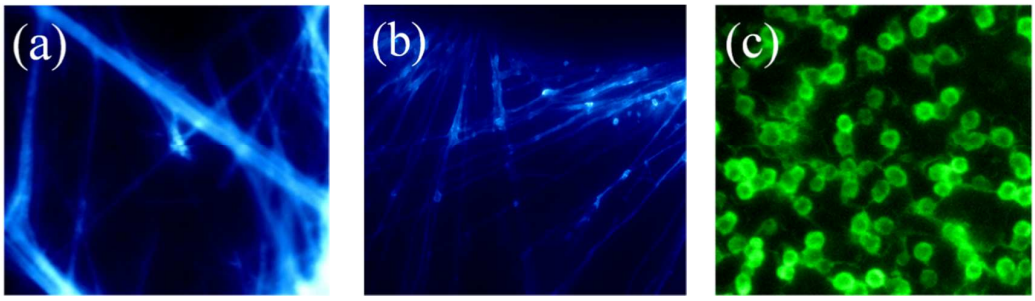

Figure 7. Fluorescence microscopy images of thermally induced a) FF, b) LL, c) FFF nanostructures. Blue PL images ("a" and "b") were obtained by excitation in UV spectral region (DAPI filter, excitation wavelength 352-402 nm, emission wavelength ~417 – 477 nm). Green image "c" was obtained by excitation using GFP filter, excitation wavelength 457-487 nm, emission wavelength ~502-538 nm

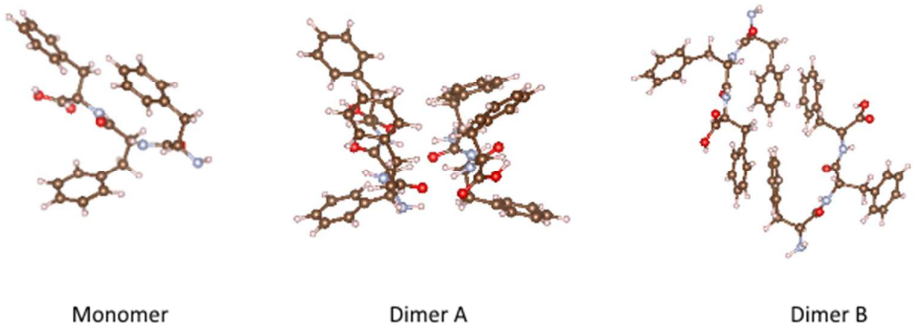

Figure 8. Ball and stick models for FFF configurations. Left – FFF monomer (one of many possible configurations), Middle – Dimer A – hydrogen bonds stabilized dimer, Right- dimer B – a dimer with two phenyl end groups in close proximity. Carbon atoms are shown in brown, hydrogen in white, nitrogen in light blue and oxygen in red.

Table 1. Summary on structure and properties of peptide nanostructures in native and thermally-induced phase[23, 24,25,30]

Peptide	**Native Phase**		**Thermally-Induced Phase**	
	Molecular State, Morphology	**Observed Physical Properties**	**Molecular State, Morphology, Peptide Secondary Structure**	**Observed Physical Properties**
FF	Linear FF, Hollow nanotubes	Piezoelectric, Nonlinear Optical, UV PL	Cyc-FF Nanofibrils β-sheet	UV PL, Visible (blue and green) PL
LL	Linear LL, Hollow nanotubes	Piezoelectric, Nonlinear Optical	Cyc-LL, Nanofibrils β-sheet	Visible (blue and green) PL
FFF	Linear FFF, Nano-spheres	Nonlinear Optical, UV PL	Linear FFF, Nanofibrils, β-sheet	UV PL, Visible (blue and green) PL
Cyc-FF	Cyc- FF, Nanofibrils	UV PL	No changes Cyc-FF, Nanofibrils β-turn	UV PL

Table of Contents Graphic

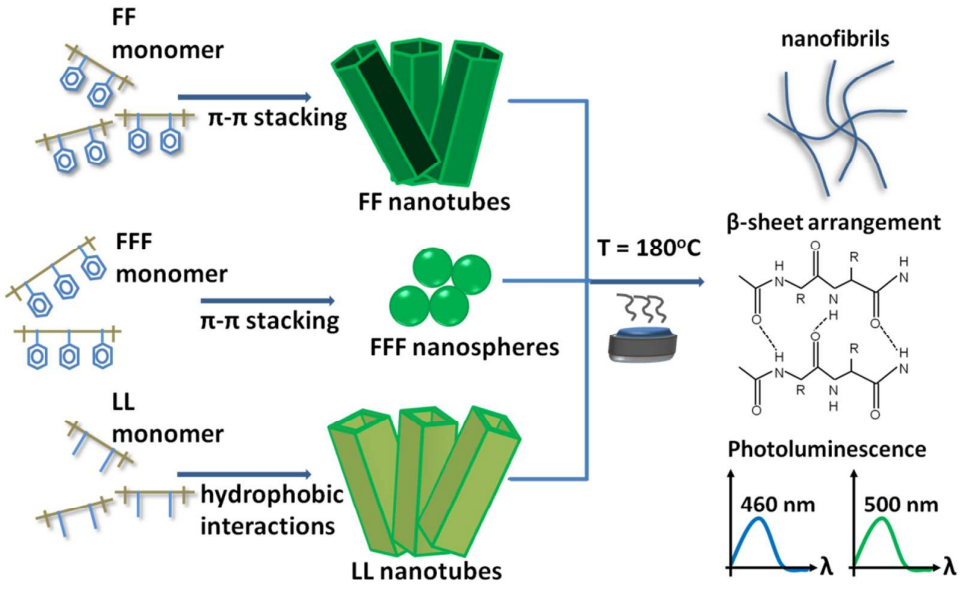

Illustration of the thermally-induced phase transition of peptide nanostructures of different native origin and shape to a new phase with similar nanofibrous morphology, having the same antiparallel β-sheet peptide secondary structure and newly acquired photoluminescence properties in the visible blue/green region which is ascribed to noncovalent hydrogen bonds of these supramolecular structures

References

[1] Lehn, J. M. Toward Self-Organization and Complex Matter. *Science*. **2002**, 295, 2400-2403.
[2] Lehn, J. M. *Supramolecular chemistry. Concepts and perspectives*. VHC: Weinheim, Germany,1995.
[3] Zhang, S. Fabrication of Novel Biomaterials Through Molecular Self-Assembly. *Nat. Biotechnol*. **2003**, 21, 1171–1178.
[4] Gao, Y.; Matsui, H. Peptide-Based Nanotubes and Their Applications in Bionanotechnology. *Adv. Mater*. **2005**, 17, 2037–2050.
[5] Gazit, E. Self-Assembled Peptide Nanostructures: The Design of Molecular Building Blocks and Their Technological Utilization. *Chem. Soc. Rev*. **2007**, 36, 1263–1269.
[6] Ulijn, R. V.; Smith, A. M. Designing Peptide Based Nanomaterials. *Chem. Soc. Rev*. **2008**, 37, 664–675.
[7] Ghadiri, M.R.; Grania, J.; Milligan, R.; McRee, D.; Khazanovitch, N. Self-assembling Organic Nanotubes Based On a Cyclic Peptide Architecture. *Nature* **1993**, 366, 324–327.
[8] Hartgerink, J.; Granja, J.; Milligan, R.; Ghadiri, M. R. Self-Assembling Peptide Nanotubes. J. *Am. Chem. Soc*. **1996**, 118, 43–50.
[9] Reches, M., Gazit, E. Casting Metal Nanowires Within Discrete Self-Assembled Peptide Nanotubes. *Science* **2003**, 300, 625–627.
[10] Amdursky, N.; Gazit, E.; Molotskii, M.; Rosenman, G. Elementary building blocks of self-assembled peptide nanotubes. J. Amer. Chem. Soc. **2010**, 132, 15632–15636.
[11] Hauser, C. A. E.; Zhang, S. Peptides as biological semiconductors. *Nature, New and Views* **2010,** 468, 516-517.
[12] Dobson, C. M. The structural basis of protein folding and its links with human disease, *Phil.Trans. R. Soc. Lond. B*. **2001**, 356, 133-145.
[13] Lowik, D. W. P. M.;. Leunissen, E. H. P; van den Heuvel, M.; Hansen, M. B; and van Hest, J. C. M. Stimulus responsive peptide based materials. *Chem. Soc. Rev*. **2010**, 39, 1–19
[14] Hamley, I. W. Peptide fibrillisation. Angew. Chem. 2007, 46, 8128−8147
[15] Ning, Du.; Liu X. Y.; Narayanan J.; Li L.; Min Lim, M. L.; Li, D. Design of Superior Spider Silk: From Nanostructure to Mechanical Properties. *Biophysical Journal*. **2006**, 91, 4528–4535.
[16] Keten, S.; Xu, Z.; Ihle, B.; Buehler, M. J. Nanoconfinement controls stiffness, strength and mechanical toughness of β-sheet crystals in silk. *Nat Mater*. **2010**, 9, 359-367.
[17] Keten, S.; Buehler, M. J. Asymptotic Strength Limit of Hydrogen-Bond Assemblies in Proteins at Vanishing Pulling . *Phys. Rev. Lett.* **2008**,100, 198301.
[18] Zhang, L.; Chen, T.; Ban, H.; Liu, L. Hydrogen bonding-assisted thermal conduction in β-sheet . Nanoscale. 2014, 6, 7786.
[19] del Mercato, L. L.; Pomp, P. P.; Maruccio, G.; Torre, A. D.; Sabella, S.; Tamburro, A. M.; Cingolani, R.; R. Rinaldi. Charge transport and intrinsic fluorescence in amyloid-like fibrils. PNAS104, 18109-18124.
[20] Chan, F. T.; Kaminski, G. S.; Kumita, J. R.; Bertoncini, C. W.; Dobson, C. M.; Kaminski, C. F. Protein Amyloids Develop an Intrinsic Fluorescence Signature During Aggregation. *Analyst* **2013**, 138, 2156–2162.
[21] Pinotsi, D.; Buell, A. K.; Dobson, C. M.; Kaminski, G. S.; Kaminski, C. F. A Label-Free, Quantitative Assay of Amyloid Fibril Growth Based on Intrinsic Fluorescence. *ChemBioChem*. **2013,** 14: 846–850.
[22] Adler-Abramovich, L.; Kol, N.; Yanai, I.; Barlam, D.; Shneck, R. Z.; Gazit, E.; and Rousso, I. Self-Assembled Organic Nanostructures with Metallic-Like Stiffnes. *Angew. Chem. Int. Ed.* **2010**, 49, 1 – 5
[23] Amdursky, N.; Beker, P.; Shklovsky, J.; Gazit, E.; Rosenman, G. Ferroelectric and related phenomena in biological and bioinspired nanostructures. *Ferroelectrics.* **2010,** 399,107-112.
[24] Kholkin, A.; Amdursky, N.; Bdikin, I.; Gazit, E.; G. Rosenman. Strong Piezoelectricity in Bioinspired Peptide Nanotubes. *ACS Nano.* **2010**, 4, 610-616.
[25] Handelman, A.; Lavrov, S.; Kudryavtsev, A.; Khatchatouriants, A.; Rosenberg, Y.; Mishina, E.; Rosenman G. Nonlinear Optical Bioinspired Peptide Nanostructures. *Advanced Optical Mater*. **2013**, 1, 875–884.
[26] Adler-Abramovich, L.; Aronov, D.; Beker, P.; Yevnin, M.; Stempler, S.; Buzhansky, L.; Rosenman, G.; Gazit E. Self-Assembled Arrays of Peptide Nanotubes by Vapor Deposition. *Nat. Nanotech*. **2009**, 4, 849-955.
[27] Bank-Srour, B.; Beker, P.; Krasovitsky, L.; Gladkikh, A.; Rosenberg, Y.; Barkay, Z.; Rosenman, G. Physical Vapor Deposition of Peptide Nanostructures, *Polymer Journal*, **2013**, 45, 494–503.

[28] Lakshmanan, A.; Zhang, Z.; Hauser, C. A.E. Short self-assembling peptides as building blocks for modern nanodevices. *Trends in Biotechnology* **2012**, 30, 155-165.
[29] Kim, S.; Kim, J. H.; Lee, J. S.; Park, C. B. Beta-Sheet-Forming, Self-Assembled Peptide Nanomaterials towards Optical, Energy, and Healthcare Applications. *Small* **2015**, DOI: 10.1002/smll.201500169
[30] Handelman, A.; Beker, P.; Amdursky, N.; Rosenman, G. Physics and Engineering of Peptide Supramolecular Nanostructures, *Perspective Review, Phys. Chem. Chem. Phys*. **2012**,14, 6391–6408.
[31] Hamley, I. Peptide Nanotubes. *Angew. Chem. Int. Ed.* 2014, 53, 6866 – 688
[32] Gatto, E.; Venanzi, M.; *Peptronics: peptide materials for electron transfer*, in book "*Peptide Materials: From Nanostructures To Applications*, Ed. by Aleman C.; Bianco A.; M. Venanzi. Wiley: **2013**, 105-144.
[33] Amdursky, N.; Gazit, E.; Rosenman, G. Quantum Confinement in Self-Assembled Bio-Inspired Peptide Hydrogels. *Advanced Materials* **2010**, 22, 2311-2316.
[34] Yan, X.; Su, Y.; Li, J.; Fruh, J.; Mohwald, H. Uniaxially Oriented Peptide Crystals for Active Optical Waveguiding. *Angew. Chem. Int. Ed*. **2011**, 50, 11186- 11191.
[35] Berger, O.; Adler-Abramovich, L.; Levy-Sakin, M.;, Grunwald A.; Liebes-Peer, Y.; Bachar, M.; Buzhansky, L.; Mossou, E.; Forsyth, V. T.; Schwartz, T.; Ebenstein, Y.; Frolow, F.;, Shimon, L. J. W.; Patolsky, F.; and Gazit, E.. Light-emitting self-assembled peptide nucleic acids exhibit both stacking interactions and Watson–Crick base pairing. *Nature Nanotech*. **2015**, 10, 353-360
[36] Amdursky, N.; Molotskii, M.; Aronov, D.; Adler-Abramovich, L.; Gazit, E.; Rosenman, G. Blue Luminescence Based on Quantum Confinement at Peptide Nanotubes. *Nano Lett*. **2009**, 9, 3111-3115.
[37] Bosne, E. D.; Heredia, A.; Kopyl,S.; Karpinsky, D. V.; Pinto, A. G.; and Kholkin, A. L. Piezoelectric resonators based on self-assembled diphenylalanine microtubes. *Appl. Phys. Lett* . **2013**, 102, 0735041-5
[38] Amdursky, N.; Shalev, G.; Handelman, A.; Litsyn, S.; Natan, A.; Roizin, Ya.; Rosenwaks, Y.; Szwarcman, D.; Rosenman, G. Bioorganic Nanodots for Non-Volatile Memory Devices. *Apl. Phys. Lett. Mat*. **2013**, 1, 062101-062106.
[39] Lee, J. S.; Ryu, J.; and Park, C. B. Bio-inspired fabrication of superhydrophobic surfaces through peptide selfassembly. *Soft Matter*. **2009**, 5, 2717–2720
[40] Kresse, G.; Furthmüller, J. Efficient iterative schemes for ab initio total-energy calculations using a plane-wave basis set. *Phys. Rev. B* **1996,** 54**,** 11169–11186.
[41] Perdew, J. P.; Burke, K.; Ernzerhof, M. Generalized gradient approximation made simple. *Phys. Rev. Lett.* **1996**, 77, 3865-73.
[42] Krukau, A. V.; Vydrov, O. A.; Izmaylov, A. F.;Scuseria, G. E. Influence of the exchange screening parameter on the performance of screened hybrid functionals. *J. Chem. Phys.* **2006**, 125**,** 224106-12
[43] Tkatchenko, A.; Scheffler, M. Accurate Molecular Van Der Waals Interactions from Ground-State Electron Density and Free-Atom Reference Data. *Phys. Rev. Lett.* **2009**, 102**,** 073005-12.
[44] Blochl, P. E. Projector augmented-wave method. *Phys. Rev. B*, **1994,** 50,17953-61. Kresse, G.; Joubert, D. From ultrasoft pseudopotentials to the projector augmented-wave method. *Phys. Rev. B*. **1999**, 59,1758-66.
[45] Gorbitz, C. H.; Nanotube Formation by Hydrophobic Dipeptides. *Chem. Eur. J.* **2001**, 7, 23-29.
[46] Rosenman, G.; Beker, P.; Koren, I.; Yevnin, M.; Bank-Srour, B.; Mishina, E.; Semin, S.; Bioinspired Peptide Nanotubes: Deposition Technology, Basic Physics and Nanotechnology Applications. *J. Pept. Sci*. **2010**, 17, 2, 75-87.
[47] Tamamis, P.; Adler-Abramovich, L.; Reches, M.; Marshall, K.; Sikorski, P.; Serpell, L.; Gazit, E.; Archontis, G.; Self-Assembly of Phenylalanine Oligopeptides: Insights From Experiments and Simulations. *Biophysical J.* **2009**, 96, 5020-5029.
[48] Han, T. H.; Ok, T.; Kim, J.; Shin, D. O.; Ihee, H.; Lee, H. S.; Kim, S. O. Bionanosphere Lithography Via Hierarchical Peptide Self-Assembly of Aromatic Triphenylalanine. *Small*, **2010**, 6, 945-951.
[49] Demirel G.; Malvadkar N.; Demirel M. C. Control of Protein Adsorption onto Core-Shell Tubular and Vesicular Structures of Diphenylalanine/Parylene. *Langmuir*, **2010**, 26, 1460-1463.
[50] Amdursky, N.. Beker, P.; Koren, I.; Bank-Srour, B.; Mishina, E.; Semin, S.; Rasing, T.; Rosenberg, Y.; Barkay, Z.; Gazit, E.; Rosenman, G. Structural Transition in Peptide Nanotubes, Biomacromolecules. **2011**,12, 1349–1354.
[51] Toledano, P.; Dmitriev, V. *Reconstructive phase transition in crystals and quasicrystals*, World Scientific: 1996.

[52] Cowley, R. A. *Structural phase transitions. Advances in Physics*. **1980**, 29, 1, 1-110
[53] Lines, M. E;., Glass, A. M. *Principles and applications of ferroelectrics and related materials*, Clarendon Press: Oxford, UK, 1977.
[54] Kittel, C. *Introduction to solid state physics*. John Wiley & Sons: USA, 2005.
[55] Reches, M.; Gazit, E. Controlled patterning of aligned self-assembled peptide nanotubes. *Nat. Nanotechnol*. **2006**, 1, 195–200.
[56] Ranjbar, B.; & Gill, P. Circular Dichroism Techniques: Biomolecular and Nanostructural Analyses-A Review. *Chemical Biology & Drug Design* . **2009**,74, 101.
[57] Stuart, B., *Biological Applications of Infrared Spectroscopy*, Wiley, Chichester, 1997.
[58] Marshall, K. E.; Serpell, L. C. Structural integrity of β-sheet assembly, *Biochemical Society Transactions* **2009**, 37, 671-676.
[59] Fasman, G. D. *Circular Dichroism and the conformational analysis of biomolecules*, Plenum Press:New York, USA, 1996.
[60] Han, T. H.; Ok, T.; Kim, J.; Shin, D. O;, Ihee, H.; Lee, H. S.; Kim, S. O. Bionanosphere Lithography Via Hierarchical Peptide Self-Assembly of Aromatic Triphenylalanine, *Small* **2010**, 6, 945-951.
[61] Gupta, M.; Bagaria, A.; Mishra, A.; Mathur, P.; Basu, A.; Ramakumar, S.; Chauhan, V. S. Self-Assembly of a Dipeptide- Containing Conformationally Restricted Dehydrophenylalanine Residue to Form Ordered Nanotubes. *Adv. Mater.* **2007,** 19, 858–861.
[62] Marchesan, S.; Easton, C. D.; Kushkaki, F.; Waddington, L.; Hartley, P. G. Tripeptide Self-Assembled Hydrogels: Unexpected Twists of Chirality, *Chem. Commun.* **2012**, 48,2195-2197.
[63] Ryu, J.; Park, C.B. High Stability of Self-Assembled Peptide Nanowires Against Thermal, Chemical, and Proteolytic Attacks. *Biotechnol. Bioeng*. **2010**, 105, 221–230.
[64] Su, H. R.; Qi, W.; Zhao, J.; He, Z. Hierarchical, Interface-Induced Self-Assembly of Diphenylalanine: Formation of Peptide Nanofibers and Microvesicles, *Nanotechnology***, 2011**, 22**,** 245609-245613.
[65] Woody, R. W.; Aromatic Side-Chain Contributions to the Far Ultraviolet Circular Dichroism of Peptides and Proteins, *Biopolymers* **1978,** 17, 1451–1467.
[66] Choi, S. J., Jeong W. J., Kang, S. K., Lee, M., Kim, E., Ryu du, Y., Lim, Y. B., Differential Self-Assembly Behaviors of Cyclic and Linear Peptides. *Biomacromolecules*. **2012**, 13, 1991−1995.
[67] Reches, M.; Gazit, E. Self-Assembly of Peptide Nanotubes and Amyloid-Like Structures by Charged-Termini-Capped Diphenylalanine Peptide Analogues. *Isr. J. Chem*. **2005**, 45, 363–371
[68] Davies, R. P. W.; Aggeli, A.; Self-Assembly of Amphiphilic β-Sheet Peptide Tapes Based on Aliphatic Side Chains. *J. Peptide Sci.* **2011**, 17,107–114.
[69] Subbalakshmi, C.; Manorama, S. V.; Nagaraj, R. Self-Assembly of Short Peptides Composed of Only Aliphatic Amino Acids and a Combination of Aromatic and Aliphatic Amino Acids. *J. Peptide Sci.,* **2012**, 18, 283–292.
[70] Kong, J.;Yu, S. Fourier Transform Infrared Spectroscopic Analysis of Protein Secondary Structures. *Acta Biochim. Biophys. Sin. (Shanghai)*. 2007, 39(8),549-59
[71] Dong, He; Hartgerink, J. D. Role of Hydrophobic Clusters in the Stability of r-Helical Coiled Coils and Their Conversion to Amyloid-like *b*-Sheets. *Biomacromolecules*. **2007**, 8, *617-623*
[72] Nienhaus, G. U. The Green Fluorescent Protein: A Key Tool to Study Chemical Processes in Living Cells. *Angew. Chem. Int. Ed.* **2008**, 47, 8992 – 8994.
[73] Lakowicz, J. R. *Principles of Fluorescence Spectroscopy*. Plenum Press: NY, US, 1983.
[74] Uversky, V. N.; Lyubchenko, Y. L. *Bio-nanoimaging: protein misfolding and aggregation*. Elsevier: UK, 2014.
[75] Shukla, A.; Mukherjee, S.; Sharma, S.; Agrawal, V.; Radha, Kishan, K. V.; Guptasarma, P. A. Novel UV Laser-Induced Visible Blue Radiation From Proteins: Scattering Artefacts or Fluorescence Transitions of Peptide Electrons Delocalized Through Hydrogen Bonding. *Arch Biochem Biophys*. **2004**, 428, 144-153.
[76] Guptasarma, P. Solution-State Characteristics of the Ultraviolet A-Induced Visible Fluorescence From Proteins, *Archives of Biochemistry and Biophysics*. **2008,** 478, 127–129.

[77] Sharpe, S.; Simonetti, K.; Yau, J.; Walsh P. Solid-State NMR Characterization of Autofluorescent Fibrils Formed by The Elastin-Derived Peptide GVGVAGVG. *Biomacromolecules*. **2011**, 12, 1546–1555.

[78] Lee, J. S.; Yoon, I.; Kim, J.; Ihe, H.; Kim, B.; Park, C. B. Self-Assembly of Semiconducting Photoluminescent Peptide Nanowires in the Vapor Phase. *Angew. Chem*., **2011**, 123, 1196–1199.

[79] Amdursky, N.; Handelman, A.; Rosenman, G.; Optical Transition Induced by Molecular Transformation in Peptide Nanostructures. *Appl. Phys. Lett*. **2012**, 100, 103701-103704.

[80] Handelman, A.; Natan, A.; Rosenman, G. Structural and Optical Properties of Short Peptides: Nanotubes-to-Nanofibers Phase Transformation. *J. Peptide Sci.*,**2014**, 20, 487–493.

[81] White, A.M. Applications of photoluminescence excitation spectroscopy to the study of indium gallium phosphide alloys. *J. Phys. D: Appl. Phys.* **1970**, **3** (9), 1322-1328.

[82] Wall, B. D; Zhou, Y.; Mei, S; Ardoña, H. A; Ferguson, A.L; Tovar, J.D.Variation of formal hydrogen-bonding networks within electronically delocalized π-conjugated oligopeptide nanostructures. *Langmuir* 2014, 30**,** 11375–85

[83] Tovar, J. D. Supramolecular construction of optoelectronic biomaterials. *Acc. Chem. Res.* **2013,** 46, 1527–37 ().

[84] Hisamatsu, S.; Masu, H.; Takahashi, M.; Kishikawa, K., Kohmoto, Pairwise, S.; Packing of Anthracene Fluorophore: Hydrogen-Bonding-Assisted Dimer Emission in Solid State." *Cryst. Growth Des.* **2015**,15, 2291–2302

[85] Zhao, G.J; & Han, K.L. Hydrogen bonding in the electronic excited state. *Acc. Chem. Res.* **2012,** 45**,** 404–13 ().

[86] Huang, G. J; Ho J.H; Prabhakar, Ch; Liu, Y.H; Peng, S.M; Yang, J.S. Site-selective hydrogen-bonding-induced fluorescence quenching of highly solvatofluorochromic GFP-like chromophores." *Org. Lett.* **2012**,14, 5034–7 (

[87] Cudazzo, P.; Gatti, M.; Rubio, A.; Sottile, F. Frenkel versus charge-transfer exciton dispersion in molecular crystals. *Phys. Rev. B.* **2013,** 88, 195152-7

[88] Kohnm, W.; Shamm, L. J.; Self-consistent equations including exchange and correlation effects. *Phys. Rev.* 1965, **140** (4A): A1133-40

[89] Jeon, J.; Mills, C. E.; Shell, M.S. Molecular insights into diphenylalanine nanotube assembly: all-atom simulations of oligomerization. *J. Phys. Chem.* **2013**. *B* 117**,** 3935–43.

[90] Guo, C.; Luo, Y.; Zhou, R.; Wei, G. Triphenylalanine peptides self-assemble into nanospheres and nanorods that are different from the nanovesicles and nanotubes formed by diphenylalanine peptides." *Nanoscale.* **2014,** 6**,** 2800–11

[91] Krukau, A. V.; Vydrov, O. A.; Izmaylov, A. F.; Scuseria, G. E. Influence of the exchange screening parameter on the performance of screened hybrid functionals. *J. Chem. Phys.* **2006**, 125**,** 224106-12

[92] Fernandez-Alberti, S.; Kleiman, V.D.; Tretiak, S.; and Roitberg, A. Nonadiabatic Molecular Dynamics Simulations of the Energy Transfer between Building Blocks in a Phenylene Ethynylene Dendrimer. *J. Phys. Chem***. A , 2009,** 113, 7535-41.

[93] Runge, E.; Gross, E. K. U. Density-Functional Theory for Time-Dependent Systems. *Phys. Rev. Lett.* **1984**, 52, 997–1000.

[94] Bethe, H.; Salpeter, E.. A Relativistic Equation for Bound-State Problems. *Phys.Rev.***. 1951**, 84 (6), 1232-42.

[95] Smith, A. M.; Williams, R. J.; Tang, C.; Coppo, P.; Collins, R. F.; Turner, M. L.; Saiani, A.; Ulijn, R.V. Fmoc-Diphenylalanine Self assembles to a hydrogel via a novel architecture based on π–π interlocked β-sheets. *Adv. Mater*. **2008**, 20, 37-41.

[96] Shimomura, O.; Johnson, FH, Saiga, Y. Extraction, purification and properties of aequorin, a bioluminescent protein from the luminous hydromedusan. *Aequorea*. *J Cell Comp Physiol.* **1962**, 59, 223–239.

[97] Chudako,v D. M.; Matz, M. V.; Lukyanov, S.; Lukyanov, K. A. Fluorescent Proteins and Their Applications in Imaging Living, Cells and Tissues. *Physiol Rev.* **2010**, 90, 1103–1163.

[98] Jaworska, M., Jeziorna, A., Drabik, E., Potrzebowski, M.J., Solid State NMR Study of Thermal Processes in Nanoassemblies Formed by Dipeptides, *J. Phys. Chem. C,* **2012**, 116, 12330−12338

Amir Handelman received his BSc and MSc degrees in Electrical Engineering in 2008 and 2011 respectively, from Tel Aviv University, where his final MSc thesis was on Fiber Bragg Grating Sensors. Recently, he finished his PhD studies under the supervision of Prof. Gil Rosenman and joined the faculty of electrical engineering in Holon Institute of Technology (HIT) as a lecturer and full faculty member. His research is focused on the physical properties of bioinspired peptide-based nanostructure materials, and especially on their linear and nonlinear optical properties.

Kuritz Natalia is a PhD student in the department of Physical Electronics, Tel-Aviv University since 2013. She received her B.Sc. in Chemistry and Biology from the Tel-Aviv University, M.Sc. in Chemistry from the Weizmann Institute of Science. Her current research interests include: Molecular Dynamics, DFT and other statistical approaches to computational chemistry.

Dr. Amir Natan is a faculty member in the department of Physical Electronics in Tel-Aviv University since 2011. He received his B.Sc. in Physics and Mathematics from the Hebrew University, M.Sc. In Electrical Engineering from Tel-Aviv University and PhD in Chemistry from the Weizmann Institute of Science. After his PhD he has worked as a post-doctorate fellow at Northwestern University. He has also worked in industry in the fields of signal processing, radar detection, and bioinformatics. He is a co-founder of Compugen Ltd., a leading company in the development of algorithms for research of the human genome. His current research interests include: DFT and TDDFT in the real space formalism, multi-scale materials simulations, oxide materials, and organic/inorganic interfaces. Dr. Natan is a member of the Sackler center for computational molecular and materials Science.

Prof. Gil Rosenman received his MSc degree in 1970 in experimental physics, his PhD degree in 1975 and Doctor of Science in 1989 (second level of PhD in Russia) both in Solid State Physics from Ural Polytechnic Institute (Yekaterinburg, Russia). In 1990 he joined Faculty of Engineering-Physical Electronics, Tel Aviv University, where he is a full professor (2000) and incumbent of the Henry and Dinah Krongold Chair of Microelectronics (2010). He is well-known for his studies of physics and

technology of ferroelectrics, ferroelectric electron cathodes, new phenomena of ferroelectric domain breakdown, ferroelectric domain engineering for new generation of lasers, and innovative research in the field of surface modification.

Recent activities of his group are focused on a new technology and physics of bioinspired peptide nanostructures resulting in observation of bioorganic nanodots towards a new generation of nanomaterials for nanophotonics, nanobiomedicine, bio-piezotronics.

Prof. Gil Rosenman supervised 20 PhD students, published more than 200 papers, 80 invited presentations and holds 30 patents. He is also the co-founder of the start-up company StoreDot Ltd., www.store-dot.com